The NIMA-like kinase Nek2 is a key switch balancing cilia biogenesis and resorption in the development of left-right asymmetry

S. Joseph Endicott[1]*, Basudha Basu[2]*, Mustafa Khokha[1,2], Martina Brueckner[1,2]

Departments of Genetics[1] and Pediatrics[2], Yale University School of Medicine
333 Cedar Street, Fitkin 426
New Haven, CT 06520
* these authors contributed equally

Development • Advance article

Abstract

Vertebrate left-right (LR) asymmetry originates at a transient left-right organizer (LRO), where cilia play a crucial role in breaking symmetry. The LRO is a ciliated structure, however, much remains unknown about the choreography of cilia biogenesis and resorption at this organ. We recently identified a mutation affecting *NEK2*, a member of the NIMA-like serine-threonine kinase family, in a patient with congenital heart disease associated with abnormal LR development. Here, we report how Nek2 acts through cilia to influence LR patterning. Both overexpression and knockdown of *nek2* in *Xenopus* result in abnormal LR development and reduction of LRO cilia count and motility, phenotypes that are modified by interaction with the Hippo signaling pathway. *nek2* knockdown leads to a centriole defect at the LRO, consistent with the known role of Nek2 in centriole separation. Nek2 overexpression results in premature ciliary resorption in cultured cells dependent on function of the tubulin deacetylase HDAC6. Finally, we provide evidence that the known interaction between Nek2 and Nup98, a nucleoporin that localizes to the ciliary base, is important for regulating cilium resorption. Together these data show that Nek2 is a switch balancing ciliogenesis and resorption in the development of LR asymmetry.

Introduction

The vertebrate left-right (LR) axis is the last body axis to be established, after the antero-posterior and dorsoventral axes. Thus, LR asymmetry presents a unique problem in embryonic axis development: it requires a mechanism to generate asymmetry, and to align it to the antero-posterior and dorsoventral axes. Symmetry across the mediolateral midline is broken by signaling events that occur at a conserved, transient, ciliated left-right organizer (LRO), referred to as the node in mammals, the gastrocoel roof plate (GRP) in *Xenopus*, and Kupffer's Vesicle in zebrafish (Blum et al., 2014; Hamada and Tam, 2014). Leftward fluid flow generated by motile cilia in the LRO is crucial for the initial break in symmetry (Nonaka et al., 1998; Schweickert et al., 2007), and reversal of this fluid flow reverses the body plan in mice (Nonaka et al., 2002). Fluid flow is thought to be sensed by a population of immotile mechanosensory cilia near the periphery of the LRO, which initiate calcium signaling events that lead to asymmetric gene expression (McGrath et al., 2003; Yuan et al., 2015). Both motile and sensory LRO cilia are primary cilia, arising directly from mother centrioles. Thus, LRO ciliogenesis and resorption are intimately linked with centrioles and the cell cycle at the LRO. While ciliogenesis defects have been extensively linked to abnormal development of LR asymmetry (Yuan et al., 2013), defects affecting cilia resorption are much less common causes of abnormal LR axis formation. Thus far, the only gene identified to be required for both cilia resorption and LR development is *Pitchfork*, which activates Aurora A to promote ciliary disassembly (Kinzel et al., 2010). Downstream of cilia-generated fluid flow and sensation, the mRNA encoding the nodal inhibitor *Dand5* (*Cerl2, charon, coco*) is degraded on the left side in response to flow (Nakamura et al., 2012; Schweickert et al., 2010). This leads to an increase in left-sided Nodal signaling. Nodal promotes its own expression, propagating across the left side, where it activates downstream asymmetric expression of

Pitx2 in the left lateral plate mesoderm (LPM) (Hamada et al., 2001; Levin et al., 1995). Laterality-specific organ morphogenesis arises subsequent to asymmetric expression of *Nodal* and *Pitx2*.

Defects in the establishment of the LR axis can result in a spectrum of malformations of the internal organs collectively referred to as heterotaxy. This condition is often accompanied by a severe category of congenital heart disease (Isao Shiraishi, 2012). Because the establishment of the LR axis is dependent upon cilia, heterotaxy has been associated with primary ciliary dyskinesia (PCD), a syndrome arising from defects in cilia motility (Kennedy et al., 2007; Li et al., 2015). Beyond PCD, mutations in additional genes required for cilia function have been identified in human heterotaxy patients (Sutherland and Ware, 2009). We previously reported analysis of copy-number variants in 262 human heterotaxy patients that identified a patient with a duplication encompassing the entire *NEK2* gene (never in mitosis kinase 2) (Fakhro et al., 2011).

Nek2 is a member of the NIMA (never in mitosis A) family of serine-threonine kinases, highly conserved across vertebrates, with roles in cell cycle and centrosome biology (Fry et al., 2012). Moreover, *nek2* is expressed in the developing *Xenopus* LRO and kidney, tissues where cilia are essential for function (Fakhro et al., 2011). Evidence from human genetics links the Nek-family serine-threonine kinases *NEK1* (Thiel et al., 2011), *NEK2* (Fakhro et al., 2011), and *NEK8* to ciliopathies (Otto et al., 2008). At the onset of mitosis, Nek2 phosphorylates the centrosomal linker proteins C-Nap1, Cep68, and Rootletin leading to centrosome disjunction, a necessary step enabling the formation of the mitotic spindle (Bahe et al., 2005; Fry et al., 1998a; Fry et al., 1998b). Consequently, overexpressing Nek2 in cells leads to premature centrosome splitting (Fry et al., 1998b). RNAi mediated knock-down of Nek2 leads to cell cycle arrest in late G_2 in mouse blastomeres (Sonn et al., 2004). Consistently, overexpression of a kinase-dead Nek2 in cultured cells results in a dominant-

negative effect that blocks centriole splitting; however, occasionally mitosis completes abnormally, with one daughter cell receiving >2 centrioles and the other receiving <2 (Faragher and Fry, 2003). Nek2-dependent centrosome disjunction is downstream of two components of the Hippo pathway: the mammalian-sterile 20-like kinase (MST2 also serine-threonine kinase 3/STK3) and the scaffold protein Salvador, which are required for Nek2 localization to the centrosome and subsequent phosphorylation of C-Nap1 and Rootletin (Mardin et al., 2010).

In addition to facilitating centriole splitting on mitotic entry, Nek2 is also required for timely disassembly of the cilium in mammalian cultured cells, and NIMA-family kinases have been implicated in cilia resorption in species as divergent from vertebrates as *Tetrahymena* and

Chlamydomonas (Moe R. Mahjoub, 2004; Wloga et al., 2006). siRNA-mediated knockdown of *NEK2* in human RPE cells leaves cells with remnants of a cilium even during the formation of a mitotic spindle, and cells overexpressing *NEK2* tend to have fewer and shorter cilia (Spalluto et al., 2012). Cilia resorption requires deacetylation of axonemal tubulin downstream of Aurora kinase activity (Pugacheva et al., 2007); interestingly, recent evidence suggests that Nek2 phosphorylates Kif24 prior to mitosis. Kif24, once activated facilitates cilium resorption by mediating microtubule depolymerization (Kim et al., 2015).

At the onset of mitosis, the nuclear envelope (NE) must be broken down, beginning with the partial disassembly of the nuclear pore complexes (NPCs). Nek2 (along with Nek6 and Nek7) plays a role in this process by phosphorylating a regulator of NPC stability, Nup98, at four of its 13 phosphorylation sites. Once phosphorylated, Nup98 disassociates from the NPC, leading to a destabilization of the NPC that precedes nuclear envelope (NE) breakdown (Laurell et al., 2011). Without Nup98, the central FG component Nup62 and several cytoplasmically oriented Nups show decreased incorporation into the NPC (Wu et al.,

2001). Furthermore, overexpression of a mutant form of Nup98, which cannot be phosphorylated by the Nek kinases, stabilizes the NPC and delays mitotic entry (Laurell et al., 2011). Noting that several NPC components have now been reported to localize to the base of the cilium or to the centrosome (Hashizume et al., 2013; Itoh et al., 2013; Kee et al., 2012), we hypothesized that Nup98 plays a role in the integrity of the cilium downstream of Nek2, similar to the way it plays a role in the integrity of the NE.

Here we address the mechanism by which Nek2 affects LR patterning. We demonstrate that both knockdown and overexpression of *nek2* in *Xenopus* embryos result in LR patterning defects. The LR defect in both instances results from a loss of LRO cilia number and motility. Loss of Nek2 results in centriole defects in *Xenopus* embryos and correlates with defects in LRO cilia biogenesis, downstream of the Hippo pathway. Furthermore, we find that in Nek2 overexpression-mediated loss of cilia in cultured cells, Nek2 acts upstream of HDAC6 to mediate ciliary resorption. Finally, we provide evidence that points to a model whereby the nucleoporins comprise a component of the cilium that must be disassembled prior to cilium resorption, and that Nek2 is capable of initiating this disassembly.

Results

nek2 knockdown and overexpression affect left-right patterning in *Xenopus*

Assessment of heart-looping at stage 45 is a commonly used metric to score for LR patterning defects in *Xenopus*. In normally looped hearts (D-loops), the outflow tract (OFT) emerges from the ventricle on the animal's right and curves leftward. In cases of abnormal LR patterning, reversals (L-loops) and unlooped midline OFTs (A-loops) can be observed (Fig. 1A). RNAi mediated knock-down of *Nek2* leads to cell cycle arrest and death in mouse blastomeres (Sonn et al., 2004), indicating that early embryos are very sensitive to Nek2 levels. Thus, we decided to take advantage of morpholino technology, which allowed us to

make a graded dosage series of knockdowns of Nek2 in *Xenopus* embryos (Fig. 3C). To ensure morpholino specificity, we used two morpholinos, targeting a splice acceptor (MO1) and a splice donor (MO2) of the *nek2* transcript, to knock down *nek2* in *Xenopus*. Nek2 has two isoforms, Nek2A and Nek2B (Hames and Fry, 2002), and both morpholinos are expected to target the transcripts to both forms. Both morpholinos caused the phenotype of a significant number of abnormally looped hearts (Fig. 1A); however, MO1 gave a stronger phenotype, and was thus used for all subsequent experiments, unless otherwise stated. A non-targeting control MO did not have any affect on heart looping. Injection of 100pg of full length human *NEK2* (*hNEK2*) mRNA is capable of rescuing the morphant phenotype, suggesting that the morpholino is specific (Fig. 1A). Because the human heterotaxy patient with a *NEK2* mutation had a copy number duplication (Fakhro et al., 2011), we hypothesized that overexpression of this gene would also cause LR patterning defects in *Xenopus*. Indeed, a dosage of 200 pg of *hNEK2* mRNA is sufficient to cause heart-looping defects (Fig. S1A). Nek2 is a kinase with a large number of substrates. We established that kinase activity of Nek2 is essential for its overexpression phenotype by injecting a kinase-dead mutant of Nek2 with a K37R mutation (Fry et al., 1995). Injection of *hNEK2*-KD did not cause any significant LR defects when injected at the same dose as the WT construct (Fig. S1B).

The knockdown and overexpression phenotypes of *nek2* arise upstream of asymmetry genes *dand5* and *pitx2*

nek2 is expressed in many tissues during development, including in tissues important for LR patterning, such as LRO, lateral plate mesoderm (st. 21), mediolateral midline (st. 21), and developing organs including the kidney (st. 27, Fig. S2A (Fakhro et al., 2011)). Thus, the role of Nek2 in LR patterning could not be predicted by its expression pattern, and we turned to other markers of LR patterning to position the function of Nek2 within the pathway.

Dand5 is the first gene known to be asymmetrically expressed downstream of LRO flow, showing decreased expression on the left (the side that receives flow) compared to the right (Schweickert et al., 2010). Dand5 suppresses nodal at the right of the LRO, preceding the establishment of the asymmetric expression domains of *nodal*, *lefty,* and *pitx2* in the left lateral plate mesoderm (Schweickert et al., 2010; Vonica and Brivanlou, 2007). These asymmetric expression patterns are highly conserved. We evaluated *pitx2* and *dand5* expression in *Xenopus nek2* morphant and overexpressing embryos. *pitx2* expression patterns were abnormal in 45% of morphants and 46% of overexpressors (Fig. 1B). *dand5* expression patterns were abnormal in 37% of morphants and 23% of overexpressors (Fig. 1C). Because *dand5* is the first gene known to show asymmetric mRNA downstream of flow, it follows that in the cases of both morphants and overexpressors, the Nek2-mediated LR defect occurs upstream of LRO flow sensation.

Cilia quantity and motility are reduced at the LROs in both *nek2* morphants and overexpressors

Based on observations that Nek2 localizes to the mother centriole (Kim et al., 2015) and that the LR phenotypes in *nek2* morphant and overexpressing embryos occur upstream of asymmetric *dand5* expression, we hypothesized that the LR phenotypes are secondary to abnormal LRO cilia. To visualize cilia number and motility, we fluorescently tagged primary cilia in *Xenopus* with Arl13b-GFP and used high-speed imaging in live LRO explants at stage 16 (Fig. 2A, D). In control explants, there were an average of 152 cilia/LRO, with 50% motile and 50% immotile (Fig. 2B-C, E, H). In *nek2* morphants, cilia count was reduced to an average of 85/LRO with only 31% of cilia being motile (Fig. 2B-C, F, I). In hNek2 overexpressors, cilia count was reduced to an average of 100/LRO with only 37% of cilia being motile (Fig. 2B-C, G, J). In *Xenopus*, the LRO takes the shape of a tear drop, with

motile cilia in the center and immotile cilia near the periphery (Boskovski et al., 2013). In both morphants and overexpressors, motile cilia remained concentrated at the center of the LRO, but more immotile cilia were intermingled in the center than in the control LROs (Fig. 2E-G). These results indicate that Nek2 has a role in controlling number and motility of LRO cilia. To further prove the specificity of our morpholinos in generating this loss of cilia phenotype, we demonstrate that injection of a 100pg of wild-type *hNEK2* construct is able to rescue loss of cilia caused by MO1, while 50pg of wild-type *hNEK2* was able to rescue the loss of cilia caused by MO2. Injection of the same dose of a kinase-dead version of *hNEK2* is unable to rescue the cilia defect in either case (Fig. S1D-E). We considered the possibility that changes in cilia number at the LRO resulting from overexpression or knockdown of *nek2* could be a result of a change in cell number, rather than a loss of cilia from the same number of cells. To examine this possibility, *Xenopus* embryos were injected unilaterally at the two-cell stage. *Xenopus* have the unique property that from the two cell stage, each of the two cells will form tissues on only one half of the mediolateral midline, allowing for side-specific injection. This provides an internal control, whereby the injected and uninjected sides can be compared. Dye-injected embryos were used as a negative control. This experiment was performed in two ways. First, cell nuclei were counted on each side, and a ratio of nuclei on the injected to the uninjected side was taken (Fig. S1C). In all cases, there was no significant change. To further control for cell number, cell boundaries were marked by a cadherin antibody, and cell numbers were counted on injected and uninjected sides (Fig. S3A-C). Once again, there was no difference in cell number between the two sides, suggesting that the loss of LRO cilia does not arise from a loss of cell number (Fig. S3E). LRO tissue is derived from superficial mesoderm, specified during gastrulation (Schweickert et al., 2007). To confirm that the Nek2 LRO phenotypes do not arise from a defect in mesoderm specification, we checked mesoderm specification during gastrulation by in situ hybridization for *wnt11*. In

both cases of *nek2* knockdown and overexpression, *wnt11* expression patterns matched controls, suggesting that the loss of LRO cilia did not arise from a defect in LRO tissue specification (Fig. S2B).

Changes in *nek2* expression also affect epidermal cilia

In order to determine whether Nek2 affects ciliary ultrastructure, we evaluated the effect of *nek2* knockdown on *Xenopus* epidermal cilia. Epidermal cilia were used as a proxy for LRO cilia, as the low density of cilia at the LRO make TEM imaging impractical. Function of epidermal cilia patches can be easily evaluated through a gliding assay: motor force generated by the beating of epidermal cilia is sufficient to allow embryos to glide across the bottom of a plastic dish, even when muscular activity is inhibited by benzocaine. Embryos at stage 27 are long and flat, allowing for the gliding efficiency of each side to be determined independently (Fig. 2K). We unilaterally overexpressed or knocked down *nek2*, allowing us to use the contralateral side as a control for gliding speed. In the case of the *nek2* MO, the ratio of distance travelled between the injected and uninjected sides was 0.21 ($p<0.05$) (Fig. 2K). In the case of hNek2 overexpression, the injected to uninjected gliding distance ratio was 0.74 ($p<0.05$).

Epidermal cilia of *nek2* morphant embryos at stage 32 were examined by SEM and TEM (Fig 2L). SEM shows reduction in the density of cilia in the *nek2* morphant embryos compared to the control epidermis (Fig. 2Li, ii). TEM reveals that the axonemal structure is normal in the *nek2* morphant embryos showing a 9+2 arrangement with inner and outer dynein arms (Fig. 2L iii,iv). The combination of reduction in ciliary number and preserved ciliary ultrastructure suggests that the gliding defect results from decreased numbers of cilia.

Centrioles in *nek2* morphants show a reduction in γ-tubulin incorporation

Based on known roles of Nek2 in centriole biogenesis and splitting and the function of the mother centriole as the basal body of the cilium, we hypothesized that the loss of cilia in *nek2* morphants may be associated with a centriolar defect. We therefore examined centrioles at the LRO of *nek2* morphants by epifluorescent microscopy, staining for γ-tubulin, which forms the structural core of the centrioles. Interestingly, when centrioles are stained for γ-tubulin, *nek2* morphants show significantly fainter staining for γ-tubulin than control embryos (Fig. 3A-B). Signal intensity was normalized relative to the background yolk autofluorescence and pigment spots. After showing that total γ-tubulin protein levels are not decreased in *nek2* morphants (Fig. 3C), we quantified the fluorescence intensity of centriole-associated γ-tubulin in the morphants and controls, showing a significant reduction in the morphants (Fig. 3D). This data is consistent with the fact that Nek2B is involved in centriole assembly in *Xenopus* egg extracts, and absence of Nek2B results in a reduction in γ-tubulin incorporation from centrioles in egg extracts (Fry et al., 2000). These data suggest that Nek2 is required for centriole biogenesis throughout development in *Xenopus*.

Nek2 is required for centriole separation at the LRO downstream of the Hippo pathway

Nek2 plays an essential role in centrosome disjunction by phosphorylating the linker proteins C-Nap1 and Rootletin (Mardin et al., 2010). This is initiated when two members of the Hippo complex, STK3 (MST2) and Salvador co-operate to phosphorylate Nek2 (Fig. 4A). We therefore examined if Hippo-mediated activation of Nek2 plays a role in LR patterning. Knockdown of *stk3* by a start-site morpholino resulted in 29% of embryos with abnormal heart looping (Fig. 4B). Also, like the *nek2* MO, *stk3* MO had a more profound effect on LR development when injected on the left side of the embryo (Fig. 4C). This suggests that STK3,

like Nek2, may act upstream of cilia-mediated LRO flow. *stk3* morphants had a significant reduction in LRO cilia (Fig. 4D, E, G); however *stk3* knockdown does not change LRO cell number (Fig. S3D-E). Loss of LRO cilia by *stk3* knockdown can be rescued by injection of 50pg human *STK3* mRNA, suggesting specificity of the morpholino (Fig. S1F). To examine whether the LRO cilia phenotype in *stk3* morphants is mediated by Nek2, we show that *hNEK2* mRNA partially rescues the LRO cilia phenotype in *stk3* morphants (Fig. 4F, G). These data point to Hippo pathway signaling, mediated by Nek2, as a predecessor to LRO cilia biogenesis.

Nek2 has been linked to centriole disjunction and biogenesis, so we evaluated centriole number at the LRO. *nek2* knockdown resulted in a significant increase in the number of LRO cells with greater than 2 centrioles (Fig. 4H-J). The Eg5 kinesin mediates centrosome separation downstream of STK3-Nek2-mediated disjunction (Mardin et al., 2010). We therefore attempted to rescue *nek2* knockdown by overexpression of *Eg5*. Co-expression of *Eg5* was found to significantly rescue the defective heart looping observed in embryos injected with a *nek2* MO (Fig. 4K), providing further evidence for the importance of Nek2-mediated centriole splitting in LRO function and LR development.

Nek2 overexpression promotes cilia resorption upstream of HDAC6-mediated tubulin deacetylation

To assess whether Nek2 overexpression leads to loss of cilia by increasing ciliary resorption or inhibiting ciliary biogenesis, we evaluated whether pharmacologic blockade of tubulin de-acetylation affects the Nek2-overexpression induced loss of cilia. Ciliary resorption is preceded by activation of Aurora A kinase at the centriole, followed by HDAC6 mediated deacetylation of tubulin in the axoneme (Pugacheva et al., 2007). To test whether Nek2 acts to disassemble cilia upstream of HDAC6, cells overexpressing Nek2 are treated with tubacin,

which has been shown to inhibit HDAC6, and evaluated for ciliation. IMCD3 cells were treated with tubacin to block tubulin deacetylation, and transfected with *Cherry-NEK2*. 24 hrs after transfection, cells were fixed and labeled with anti-acetylated tubulin to identify cilia and anti-DS red to detect transfection. In order to ascertain the effectiveness of tubacin in inhibition of serum-mediated cilia resorption, a subset of mock-transfected cells were then serum-fed and fixed 12 hrs later and again evaluated for ciliation (outlined in Fig. 5A). As previously shown in Nek2-overexpressing cultured retinal pigmented epithelium (hTERT-RPE1) cells (Spalluto et al., 2012), transfection with *Cherry-NEK2* leads to loss of cilia. Notably, Nek2-mediated loss of cilia is almost completely rescued by culturing the cells in tubacin-containing medium (Fig. 5B, and Fig. S4B). The level of ciliary resorption in response to Nek2 overexpression approximates that observed in response to serum feeding, and as expected serum-induced ciliary loss is also rescued by tubacin (Fig. 5C). Because of the known role of Aurora A upstream of HDAC6, we assessed Aurora A phosphorylation in Nek2 overexpressing cells. There was no difference in Aurora A phosphorylation levels between Nek2-overexpressing and control IMCD3 cells (Fig. S4A). These data indicate that overexpression of Nek2 leads to increased ciliary resorption. Further, Nek2 functions upstream of, or in parallel with, HDAC6 mediated tubulin deacetylation without affecting Aurora A phosphorylation.

Nek2-mediated cilia resorption depends on the nucleoporin Nup98

Nek2-mediated phosphorylation of Nup98 is a key step in nuclear envelope breakdown at mitotic onset (Laurell et al., 2011). The recent discovery of a role for nucleoporins in gating the base of the cilium led us to hypothesize that Nup98 may play a role in cilium integrity, similar to its role in NE integrity. We observed that Nup98 localizes near the base of the cilium, proximal to the mother centriole, by immunostaining in hTERT

RPE cells (Fig. 6A). Moreover, the localization of Nup98 at the mother centriole overlaps with the localization of Nek2 (Fig. 6B). It has been reported that a phosphomimetic Nup98 construct shows a reduced incorporation into the NPC (Laurell et al., 2011). We sought to address if the phosphorylation state of Nup98 would also influence its ability to localize to the base of the cilium. Thus, we generated a GFP-tagged Nup98 construct phosphomimetic (PM, serine to glutamate) for the four sites targeted by the Nek kinases (Laurell et al., 2011)(S494, S591, S822, S861). We also generated a phosphodead (PD, serine to alanine) construct for these four sites. When overexpressed in IMCD3 cells, PD Nup98 localized to the base of the cilium with a frequency significantly greater than that of the PM Nup98 construct (Fig. 6C-D).

Based on observations that several nucleoporins localize to the base of the cilium/centrioles (Hashizume et al., 2013; Itoh et al., 2013; Kee et al., 2012), and that Nup98 is an important regulator of NPC and NE stability, we hypothesized that Nup98 may also play a key role in regulating the stability of the nucleoporin-containing complex at the base of the cilium, and the cilium as a whole. To address this hypothesis, we generated stable lines in IMCD3 cells expressing both PD and PM Nup98. We then overexpressed Cherry-Nek2 in these lines to determine if PD Nup98 could rescue cilia loss in the face of Nek2 overexpression. Indeed, the parent line and the line expressing PM Nup98, showed 16% and 19% reductions in cilia count in response to Cherry-Nek2 overexpression, respectively; however, the line expressing PD Nup98 showed only a 1% reduction in cilia count (Fig. 6F). All three lines had the same transfection efficiency (Fig. S5A,D). Cherry-Nek2-overexpressing cells did not have different mitotic indices from the mock-transfected controls, as measured by PH3 staining (Fig. S5B). To confirm that the rescue of cilia loss by PD Nup98 is not an artifact of any genomic changes due to transgene integration, we confirmed that two other stable cell lines expressing PD Nup98 are also able to rescue, while

another line expressing PM Nup98 is not (Fig. S5C,D). Taken together, these data suggest that Nup98 is capable of stabilizing the cilium against Nek2-mediated resorption (Fig. 6E).

Discussion

In this study, we have characterized the role of the heterotaxy-associated gene *NEK2* in governing the lifecycle of the cilium at the LRO. Our results point to a model wherein Nek2 plays an important role in the lifecycle of the cilium at a minimum of four points (Fig. 7). First, Nek2 contributes to γ-tubulin recruitment to the centriole during its biogenesis. Second, Nek2 is required for centriole splitting, ensuring proper centriole inheritance. Third, Nek2 acts upstream of the HDAC6 pathway to promote tubulin deacetylation. Finally, Nek2 promotes the disassembly of the CPC, an obligate step in cilium resorption. Dosage levels of Nek2 are key to the life-cycle of the cilium: both increases and decreases in Nek2 levels result in cilia loss. Loss of Nek2 results in defective centriole biogenesis and splitting, so that cilia are never built. Overexpression of Nek2 results in aberrant phosphorylation of ciliary Nup98 and premature cilia resorption through the HDAC6 pathway.

Our finding that there is a reduction in γ-tubulin incorporation into centrioles in *nek2* morphants, despite no change in total γ-tubulin levels is consistent with previous work. Nek2B, encoded by a splice variant of *nek2*, has been shown to be required for normal γ-tubulin recruitment to centrioles in *Xenopus* zygotic extracts (Fry et al., 2000); however, this has not been followed up with *in vivo* work until now. A number of components of the distal and sub-distal appendages of the mother centriole, which branch off the γ-tubulin core (and in many cases, bind directly to γ-tubulin), are essential for cilium biogenesis (Brito et al., 2012; Cajanek and Nigg, 2014; Ishikawa et al., 2005). Thus, it follows that a loss of γ-tubulin from the mother centriole would preclude cilium biogenesis.

The role of Nek2 in triggering centriole splitting is well appreciated (Bahe et al., 2005; Fry et al., 1998b; Man et al., 2015), and our finding that LROs of *nek2* morphant embryos display some cells with multiple centrioles is reminiscent of what is seen when dominant-negative kinase-dead Nek2 is overexpressed in cell culture (Faragher and Fry, 2003). Recently, it was found that overexpression of Cep85, a novel inhibitor of Nek2A, inhibits centrosome disjunction, arresting the cell cycle, but only when Eg5 activity is blocked by pharmacological inhibition. Thus, decreased Nek2 activity can be compensated for by Eg5 activity, consistent with our finding that overexpression of Eg5 rescues the heart looping phenotypes caused by *nek2* morpholino knockdown. After the completion of mitosis, if one daughter cell receives >2 centrioles, then the other receives <2; cells missing centrioles can progress through G_1, but must synthesize new centrioles *de novo* through the Polo-like kinase 4 (Plk4) pathway before re-entering the cell cycle (Eckerdt et al., 2011; Uetake et al., 2007). LRO cells are mitotically inactive, so it is likely that the cells that inherit <2 centrioles do not synthesize new ones, and thus do not produce cilia. Knocking down Hippo pathway effector STK3 reduces the number of LRO cilia, yet this is partially rescued by injection of *hNEK2*. Our data support a model where the Hippo pathway acts upstream of ciliogenesis by insuring proper inheritance of centrioles.

Thus, we propose that the phenotype of *nek2* morphants results from the combination of effects from both asymmetric inheritance of centrioles and a reduction in γ-tubulin incorporation into centrioles. In both cases, cells are left without a properly mature mother centriole capable of forming a cilium.

Cilium resorption requires the activation of the kinase, Aurora A, which phosphorylates tubulin deacetylase HDAC6 (Kim et al., 2014; Pugacheva et al., 2007). One function of HDAC6 is to remove acetyl marks from axonemal tubulin, contributing to the destabilization and disassembly of the axoneme (Hubbert et al., 2002; Pugacheva et al.,

2007). Nek2 is also required for timely resorption of the cilium at the G_2/M transition, and overexpression of Nek2 causes premature resorption of cilia (Spalluto et al., 2012). We found that the HDAC6 inhibitor tubacin blocks Nek2-mediated cilia resorption, suggesting that Nek2 acts upstream of HDAC6 in cilia resorption. Intriguingly, it has previously been noted that in Nek2 overexpressing cells, Aurora A activation is normal, despite a reduction in ciliation and cilium length, suggesting that Nek2 acts either downstream or parallel to Aurora A (Spalluto et al., 2012). Aurora A interacts directly with HDAC6 (Kim et al., 2014), and is regulated by a variety of sources, including: HEF1, Pitchfork, TPX2, and Ran (Bayliss et al., 2003; Kinzel et al., 2010; Pugacheva et al., 2007; Trieselmann et al., 2003), thus we also investigated whether Aurora A is activated by Nek2. We confirmed that there was no change in Aurora A phosphorylation in response to Nek2 overexpression, consistent with published data that Nek2 does not affect Aurora A activation (Spalluto et al., 2012). Recently, it was found that Nek2 promotes cilium resorption through activation of Kif24, which mediates cilium resorption through a microtubule dependent mechanism (Kim et al., 2015). Because deacetylation of tubulin decreases microtubule stability, it is likely that tubulin deacetylation through the Aurora A/HDAC6 pathway precedes microtubule disassembly through the Nek2/Kif24 pathway. Cilium resorption appears to be a very dynamic process in which pushing or pulling at one pathway may be enough to tip the balance toward resorption or homeostasis. Thus, blocking HDAC6 with tubacin very likely mitigates the effects of having an increase in Kif24 activation. Moreover, we present evidence that nucleoporins stabilize the cilium against resorption, perhaps by gating some of the numerous factors involved in disassembly.

It has been proposed that nucleoporins localize to the base of the cilium to form a complex that fulfills a role similar to that of the NPC, possessing activity as both a diffusion barrier and a regulator of directional import into the cilium (Kee et al., 2012; Takao et al.,

2014). Many GFP-tagged nucleoporins localize to the base of the cilium, and introduction of inhibitors of NPC diffusion perturb the size-exclusion permeability barrier at the base of the cilium (Kee et al., 2012). Moreover, forced dimerization of Nup62 perturbs the directional trafficking of cytosolic proteins into the cilium, but has no effect on membrane proteins (Takao et al., 2014). Studies by other groups have shown functional roles for the nucleoporins Nup62 and Nup188 at the centrosome, which contributes its mother centriole to form the ciliary basal body (Hashizume et al., 2013; Itoh et al., 2013). Tantalizing evidence that RanGTP localizes to the axoneme and that nuclear import factor Importin-β2 is required to import multiple ciliary proteins is consistent with the hypothesis that nucleoporins at the cilium may regulate directional transport of proteins into and out of the ciliary matrix, in addition to functioning as a general diffusion barrier (Dishinger et al., 2010; Hurd et al., 2011).

Nek-mediated phosphorylation of Nup98 is a key step in nuclear envelope breakdown at G_2/M (Laurell et al., 2011). The recent discovery of a role for nucleoporins in gating the base of the cilium led us to hypothesize that Nup98 may play a role in cilium integrity, similar to its role in NE integrity. It is noteworthy; however, that there are two waves of deciliation during the cell cycle (observed in RPE, IMCD3, NIH 3T3, and Caki-1 cell lines) (Li et al., 2011; Pugacheva et al., 2007; Tucker et al., 1979). First, cilia are resorbed at S-phase entry, return sometime around G_2 entry, and are then resorbed again at the G_2/M transition. During both waves of deciliation, cells show an increase in HEF1 and phosphorylation of Aurora A (Pugacheva et al., 2007). Interestingly, S-phase cilia resorption specifically requires Tctex-1, a cytoplasmic dynein associated protein (Li et al., 2011); however, much work is needed to understand the differences in the mechanisms through which the G_1/S and G_2/M waves of cilia resorption are regulated. We demonstrate localization of Nup98 to the nuclear envelope and the base of the cilium by immunostaining

with a primary antibody in addition to a GFP tagged construct. Analogous to Nup98 at the NPC, the phosphorylation state of Nup98 influences its ability to localize to the base of the cilium. Given that a PD version of Nup98 stabilizes the NPC and the NE to an extent that it delays mitotic entry, we propose that by analogy, PD Nup98 stabilizes the ciliary nucleoporin complex and the cilium against Nek-mediated breakdown. Our data are consistent with the hypothesis that removal of Nup98 from the ciliary nucleoporin complex is an obligate step in Nek2-mediated ciliary resorption. Taken together with the finding that cilia resorption is greatly delayed in cells transfected with Nek2 siRNA (Spalluto et al., 2012), our data point to a model whereby the ciliary nucleoporin complex is a component of the architecture of a cilium that is disassembled prior to cilium resorption, and that Nek2 is capable of initiating this disassembly and leads us to speculate that Nek2-mediated phosphorylation of Nup98 integrates cilia resorption and NE breakdown at G_2/M.

Observations in zebrafish demonstrate that cilia at the emerging LRO are initially immotile, and a subset of these cilia gradually become motile during the lifespan of the LRO (Yuan et al., 2015). Moreover, this gradual increase in cilia motility over time is reflected in the production of fluid flow in *Xenopus* (Schweickert et al., 2007). Interestingly, we note that in addition to loss of cilia at the LROs of *nek2* morphants and overexpressors, there was also a loss of motility of the remaining cilia in both cases. We hypothesize that *nek2* knockdown leads to defective ciliary biogenesis, resulting in cilia that never progress to a mature, motile state. In contrast, in embryos overexpressing Nek2, cilia are resorbed prematurely and are unable to maintain a proper complement of motility machinery. Future experiments are needed to address the mechanisms that contribute to this loss of motility.

The cells at the LRO coordinately generate motile primary cilia during a very brief developmental window at late gastrulation (Nonaka et al., 1998; Sulik et al., 1994; Supp et al., 1999; Supp et al., 1997). LRO cells then become mitotically inactive, while surrounding

endoderm and mesoderm continue to proliferate (Bellomo et al., 1996; Sulik et al., 1994). The requirement for exceptionally tight control of coordinating ciliary biogenesis and the cell cycle specifically at the LRO may explain why the development of LR asymmetry is so exquisitely sensitive to the dosage of Nek2, so that overexpression can manifest as abnormal laterality while preserving the remainder of development enough to develop to a living patient. By embracing a line of inquiry in which we connect single human mutations to disease pathogenesis, we have been able to extend our understanding of how the cell-cycle kinase Nek2 affects vertebrate development on a whole-organism level.

Materials and Methods

Frog husbandry

X. tropicalis were housed and cared for in our aquatics facility according to established protocols that were approved by Yale IACUC.

Xenopus knockdown and overexpression

Morpholino oligonucleotides or mRNAs were injected into 1-cell or 2-cell stage *Xenopus tropicalis* embryos as previously described (Khokha et al., 2002). The following morpholino sequences were used:

Mst2/Stk3 start site (CTAGCTTCCAATTACCCTAAAGACA)

Nek2-donor (GCTTTCTGTTGGCTCTCATACCTTT) (MO2)

Nek2-acceptor (GGCGTCTGGAATATACATGGAATTA) (MO1)

Negative control/Non-targeting (AAACCCGGGTTTACG)

Alexa488 (Invitrogen) or mini-ruby (Invitrogen) were mixed with morpholinos as tracers. mRNA transcripts were synthesized with mMessage mMachine kits (Ambion), according to the manufacturer's instructions. Full length human Nek2 including UTRs (MGC:49922) is in

a pCMV.Sport.6 backbone. xNek2A (GenBank: BC066785.1) was cloned into a GATEWAY destination vector resulting in a N-terminal GFP tag. XNek2B was cloned from stage 15 *Xenopus tropicalis* cDNA and GATEWAY cloned similar to XNek2A. his-Eg5 plasmid was a gift from Thomas Surrey, EMBL (Cahu et al., 2008). Eg5 was sub-cloned into pCS108 for RNA expression.

Antibodies

Acetylated Tubulin (Sigma: T6793); Arl13b (NeuroMab: N295B 6); Nup98 (Cell Signalling: 2596S); Nek2 (Santa Cruz: sc-55601); Ninein (Santa Cruz: sc-50142); γ-tubulin (Sigma: T6557); GFP (Life Technologies: A11122); Phospho-Histone 3 (Millipore: 06-570); anti-DS red (Clontech: 632496); E-Cadherin (BD Biosciences: 610181)

Cardiac looping in *Xenopus*

Embryos at stage 45 were paralyzed with benzocaine and positioned to expose the ventral side under a light dissection microscope. The looping of the heart is defined by the configuration of the outflow tract (OFT) with respect to the ventricle of the heart: OFT to the right (D-loop), OFT to the left (L-loop), OFT centered (A-loop).

mRNA and protein visualization in embryos

For *Xenopus* LRO immunofluorescence and *in situ* hybridization, stage 16 embryos were collected and LROs were dissected as described in (Blum et al., 2009). *In situ* hybridization was performed as described (Khokha et al., 2002) using digoxigenin labeled (Roche) probes, as described (Boskovski et al., 2013). For acetylated tubulin staining, embryos were fixed for 1 hour at room temperature in 4% paraformaldehyde. For γ-tubulin staining, embryos were fixed for 1 hour at room temperature in 4% paraformaldehyde, and re-fixed for 24 hours in

ice-cold methanol. Following rehydration, embryos were immunostained as described (Khokha et al., 2002) and mounted in Prolong Gold.

Live imaging at *Xenopus* LRO and cilia motility analysis

Experiments were performed as reported previously (Boskovski et al., 2013). Briefly, imaging was performed on a Zeiss LSM 710 DUO using a rapid LIVE linescan detector, and a 40X C-Apochromat water objective. Images were recorded across multiple Z-planes of the LRO with maximum pinhole settings, 512x512 resolution, and bi-directional scanning. There were two exceptions to our previously reported method: *arl13b-eGFP* was microinjected in place of *arl13b-mCherry* to label LRO cilia, and images were captured at a frame rate of 80 frames/second. Motility analysis was performed as detailed in (Boskovski et al., 2013).

Gliding Assays

Embryos were injected unilaterally at the two cell stage with either 4ng Nek2 MO1 or 100pg of *hNEK2* mRNA along with 50pg GFP mRNA as a tracer. At stage 27, these embryos were placed in a Petri dish, and muscle contractions were inhibited with benzocaine. Their movement was captured at 15 second intervals for 10 minutes. Gliding was measured for both the injected and uninjected side of each embryo. The movement distance of the embryo was measured by tracking the eye of the tadpole using ImageJ software.

Electron microscopy

Stage 27 *Xenopus* embryos were fixed with Karnovsky fixative for 1 h at 4°C, washed with 0.1 M sodium cacodylate, pH 7.4, then post-fixed with Palade's osmium for 1 h at 4°C, shielded from light. Following a second wash, embryos were stained with Kellenburger's solution for 1 h at RT, washed in double distilled water, then put through an ethanol series,

propylene oxide, 50/50 propylene oxide/epon, then two incubations in 100% epon. Embedded embryos were sectioned at 400 nm before staining with 2% uranyl acetate. Micrographs were taken on a Zeiss 910 electron microscope.

Fluorescence quantification of centriolar γ-tubulin

Embryos injected with 4ng of Nek2 MO1 and uninjected controls were fixed, and LROs were removed by dissection and immunostained simultaneously under identical conditions for γ-tubulin. All LROs were imaged on the same day by epifluorescent microscopy using identical settings and exposure times on a Zeiss Axiovert200M. Five LROs were selected from each group with the most similar levels of background noise (background is from yolk autofluorescence). Pigment granules appear as dark spots blocking the autofluorescence of the yolk. The same region of each LRO, slightly anterior to the blastopore, was selected for further analysis. Fluorescence intensity of γ-tubulin spots relative to the background and pigment spots was quantified using ImageJ software. No image processing, other than cropping, was applied at any stage of this experiment.

Cell culture

Mouse IMCD3 and hTERT RPE1 cells were cultures in DMEM:F12 with 10% FBS, under standard conditions. Cells were transfected with Lipofectamine 2000 (Life Technologies) by manufacturer's instructions. IMCD3 cells (in Fig 5) were fixed with 4% PFA for 10 minutes before immunostaining. hTERT RPE cells (Figure 6) were washed for 30 seconds in 0.1% saponin (to decrease background signal), before fixation with ice-cold methanol for 10 minutes. Tubacin (Sigma) was added to cell culture medium at a final concentration of 2μM.

Immunostaining of cultured cells and cilia counting.

Fixed cells were permeabilized with 0.2% Triton X in PBS, and blocked with 3% bovine serum albumin. Antibody dilutions are as follows: AcTub (1:1000), Arl13b (1:200), Nup98 (1:200), Nek2 (1:500), Ninein (1:500), GFP (1:500), Phospho-Histone 3 (1:500), anti-DS red (1:200). For cilia counting, four fields on two separate coverslips were imaged for each condition (>300 cells/condition), and the experiment was performed in triplicate. A z-stack encompassing the entire cell layer including cilia was acquired with a 63X lens on a Zeiss Axiovert microscope equipped with Apotome optical interference. The Z-stack was reconstructed as a 3-D image, and the reconstructed images of Hoechst-stained nuclei and acetylated-tubulin labeled cilia were analyzed using ImageJ software.

Acknowledgements

We would like to thank Shiaulou Yuan and Svetlana Makova for technical assistance with live-imaging experiments. We thank Michael Slocum and Sarah Kubek for frog husbandry.

Funding

This work was supported by NIH grant 1R01HL093280 to M.B., NIH grant 1R01HL124402 to M.B. and M.K., and a Brown-Coxe fellowship to B.B.

Author Contributions

S.J.E. planned and performed experiments, performed data analysis, constructed the figures and wrote the paper. B.B. planned and performed experiments and contributed to data analysis and manuscript preparation. M.K. conceived the project and planned experiments. M.B. conceived the project, planned and performed experiments, contributed to data analysis and manuscript preparation.

Figures

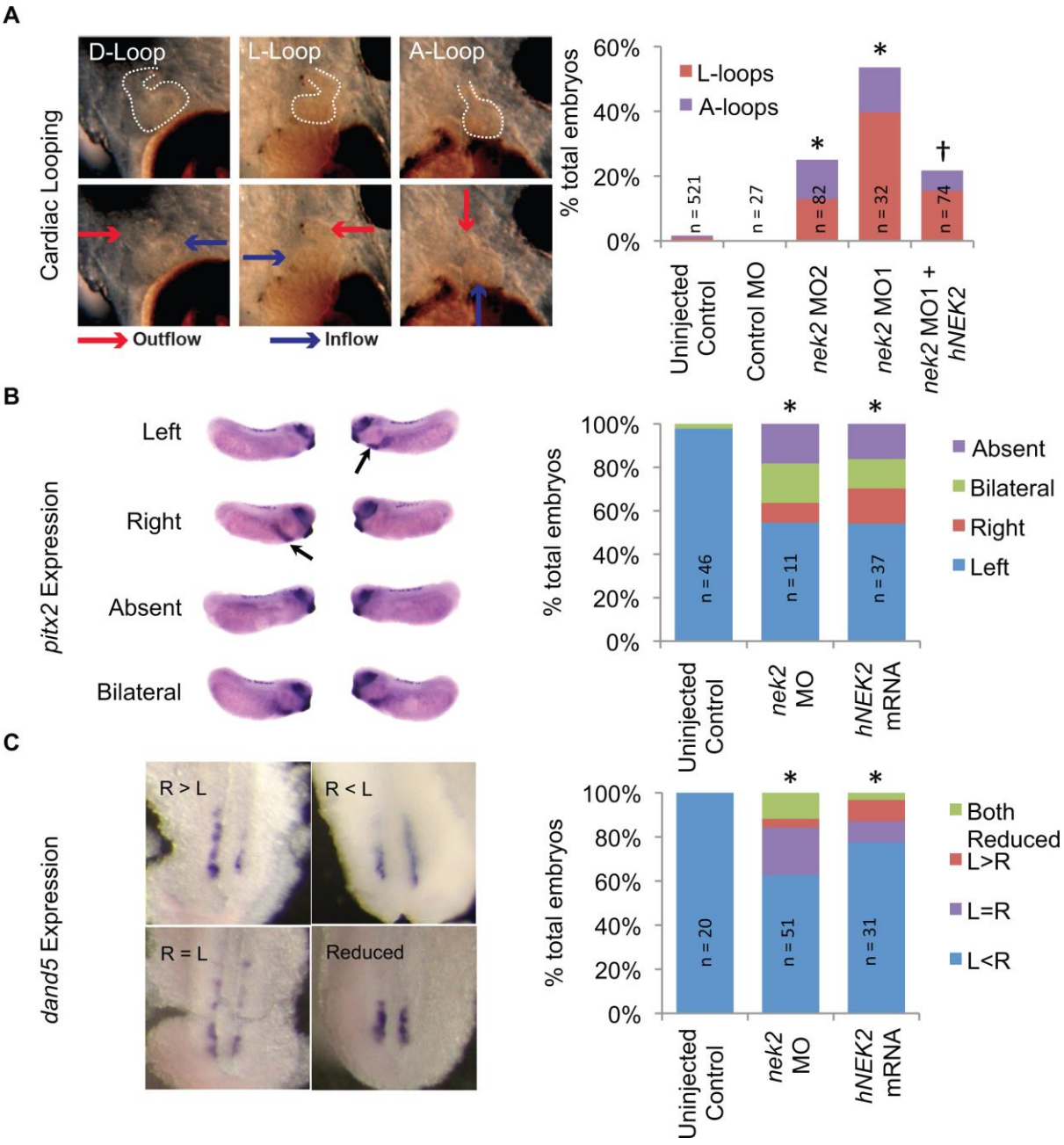

Figure 1. Nek2 affects LR patterning. (A) Knockdown of *nek2* by two different MOs causes heart-looping defects, co-injection with *hNEK2* mRNA rescues. (B) Both overexpression and morpholino knockdown of *nek2* lead to abnormal expression patterns of the laterality gene *pitx2* in the LPM. Arrows point to asymmetrically expressed pitx2 in the anterior LPM. (C) Both overexpression and morpholino knockdown of *nek2* cause

perturbation of the normal distribution of *dand5* mRNA at the LRO. *Chi-square p-value is <0.01 when compared to controls. † Chi square p-value is <0.01 when compared to MO1.

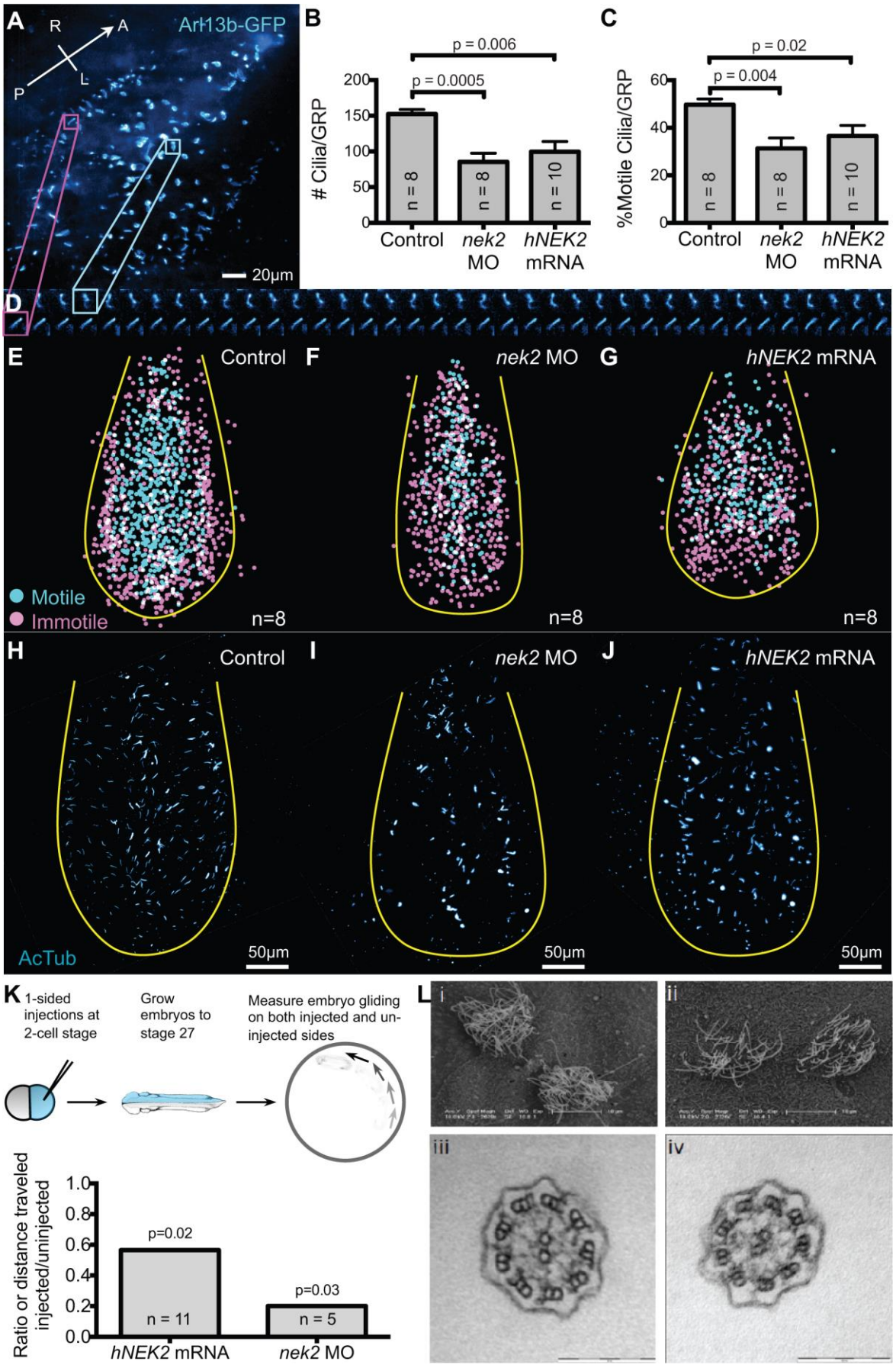

Figure 2. Both overexpression and knockdown of *nek2* lead to loss of cilia numbers and motility at the LRO. (A) Z-projection of control LRO during live imaging. A motile cilium is highlighted in cyan; an immotile cilium is highlighted in magenta. (B) There is a reduction of cilia from LROs of *nek2* morphants and overexpressors. (C) The percent of motile cilia is significantly reduced in both *nek2* morphants and overexpressors. (D) Montage of images of motile and immotile cilia over time from (A). (E-G) Maps of the distribution of motile and immotile cilia at the *Xenopus* LRO. Despite the loss of motile cilia, the distribution of motile cilia is not changed in *nek2* morphants and overexpressors. Each map is a composite of the first 8 LROs analyzed. (H-J) Acetylated tubulin stainings of LROs showing the loss of cilia in *nek2* morphants and overexpressors. (K) Nek2 expression levels affect epidermal cilia. The side of a *Xenopus* embryo injected with either *hNEK2* mRNA or *nek2* MO glides significantly less than the control side, suggesting a loss of cilia motility. (L) SEM (i-ii) and TEM (iii-iv) images of epidermal cilia from control (i, iii) and *nek2* morphant (ii, iv) embryos. Error bars are S.E.M. p values were calculated by Student's t-test for (B, C). For (K), p values are calculated by paired t-test of distance travelled between the injected and uninjected sides of the embryo.

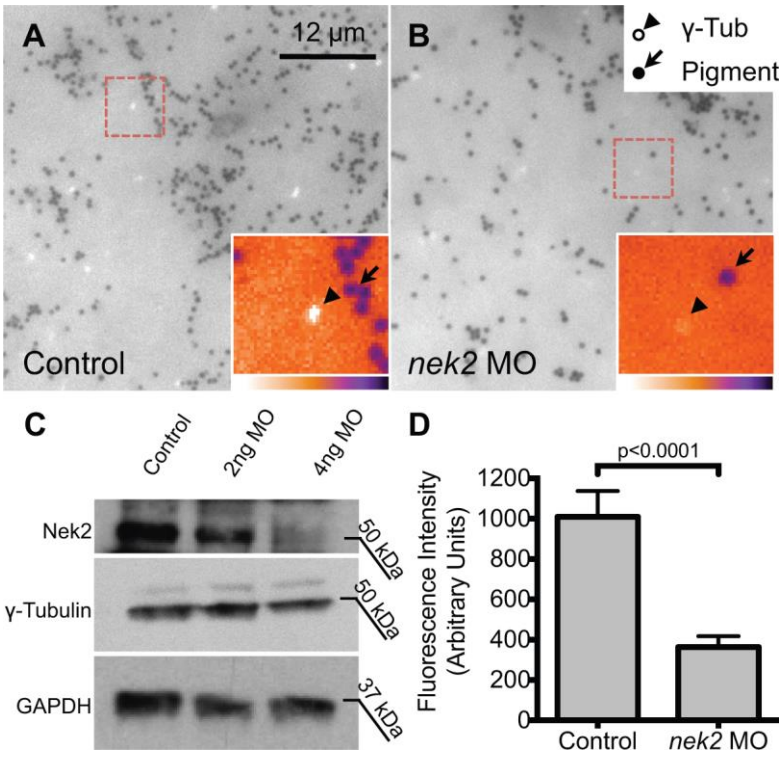

Figure 3. There is reduced γ-tubulin incorporation into centrioles at the LRO in *nek2* morphants. (A,B) Raw epifluorescent images showing LRO explants stained for γ-tubulin (light spots); dark spots are pigment granules. Insets are magnifications of boxed areas false colored as heat maps. Heat map scale at bottom of inset. (C) *nek2* morphants show a clear decrease in Nek2 protein levels, but do not show a decrease in γ-tubulin protein levels. (D) Quantification of the fluorescence intensity of centrioles of controls and morphants. Five centrioles from sections with comparable background fluorescence from five different embryos for each group were quantified. Error bars are S.E.M. p values were calculated by unpaired Student's t-test.

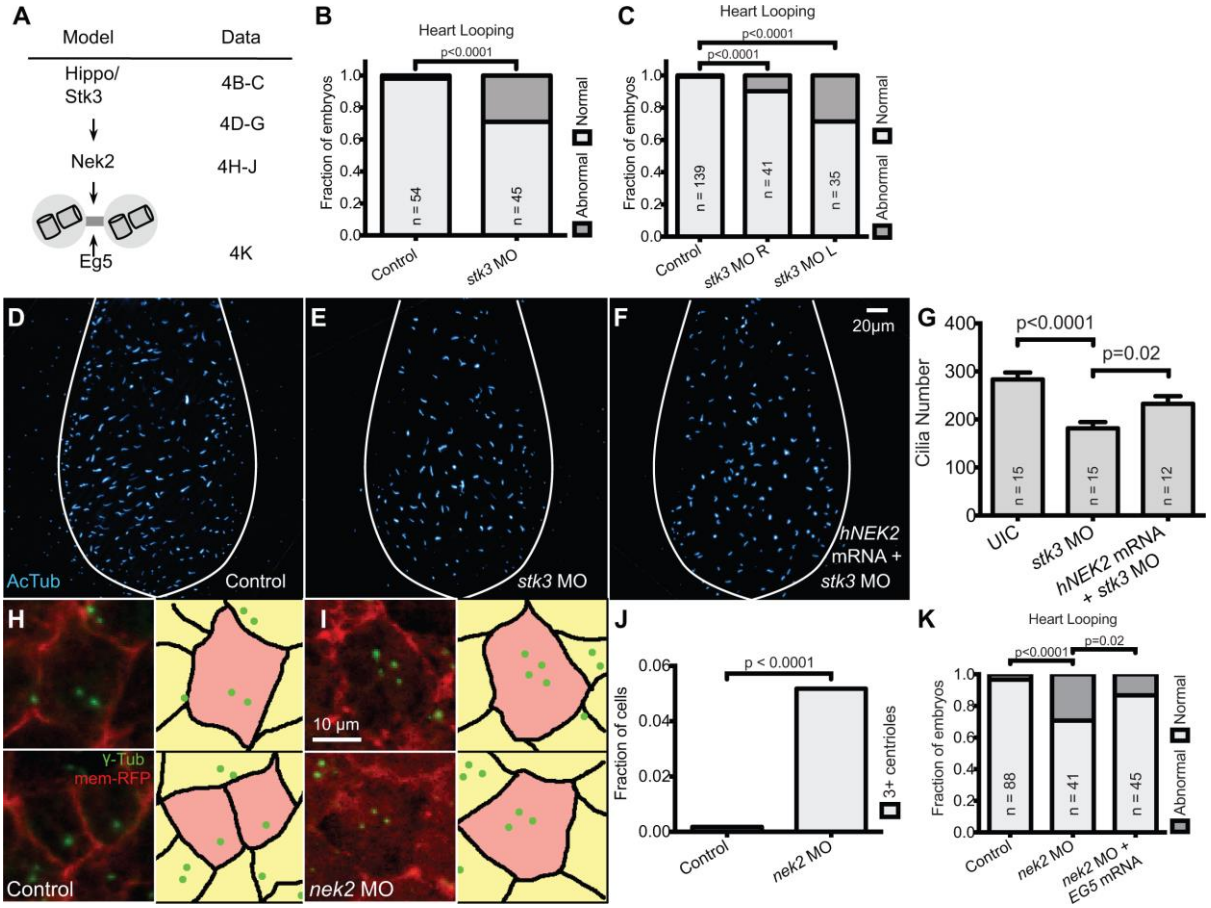

Figure 4. The interaction of Nek2 with the Hippo pathway influences cilia number at the LRO. (A) Model of how Nek2 and the Hippo pathway influence centriole splitting upstream of ciliogenesis. (B) Knockdown of *stk3* in *Xenopus* results in abnormal heart-looping. (C) When *stk3* is knocked-down on the left, it creates a much stronger phenotype than when knocked-down on the right, consistent with an LRO cilia phenotype. (D-F) Images of LRO explants stained for acetylated-tubulin to show loss of cilia in *stk3* morphants and rescue of the morphants when *hNEK2* is injected. (G) Knockdown of *stk3* causes a significant loss of LRO cilia, which is partially rescued by injection of *hNEK2*. (H, I) Representative images (left panels) and schematics (right panels) of LRO cells displaying centriole numbers. (J) *nek2* morphants have a significantly higher fraction of cells with 3 or more centrioles than controls. The centrioles of 6 LROs were counted for each condition. Between 76 and 105

cells were counted in each LRO. (K) Injection of *EG5* is able to partially rescue heart-looping in *nek2* morphants. For (B,C,J,K), p-values were calculated by χ^2 test. For (G), error bars are S.E.M. and p-values were calculated by Student's t-test.

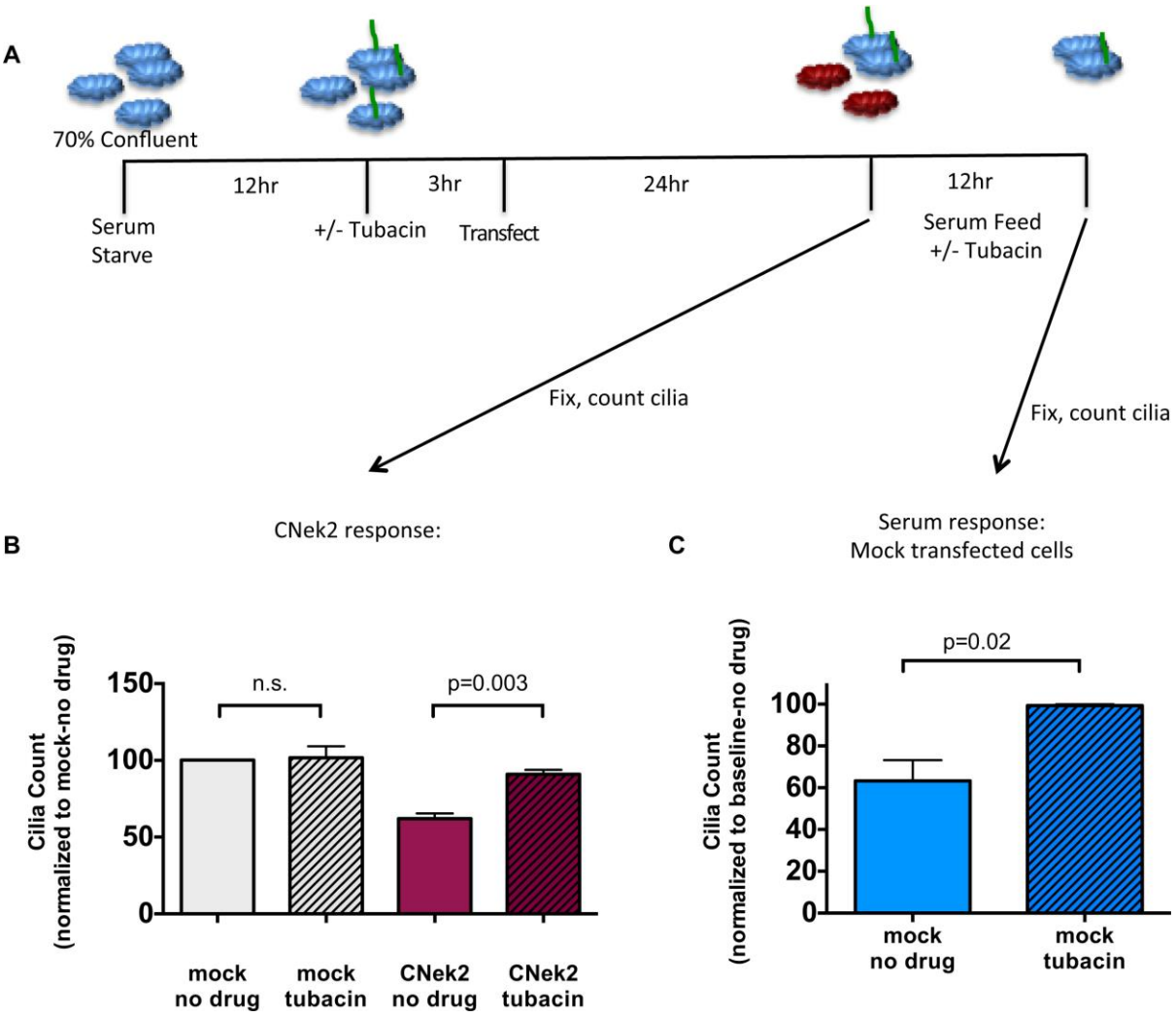

Figure 5. Nek2 affects ciliary resorption upstream of HDAC6. (A) Time line for the evaluation of ciliary resorption in response to tubacin, indicating timepoints of addition of 2μM tubacin, transfection with *Cherry-NEK2,* serum addition and cilia analysis. Mock transfected cells are shown in blue, *Cherry-NEK2* transfected cells are shown in magenta. (B) 2μM tubacin effectively blocks Nek2-mediated ciliary resorption. Data shown is the ratio of ciliated cells in transfected cells relative to mock transfected cells 24 hrs after transfection. (C) 2μM tubacin effectively blocks serum-induced ciliary resorption in mock transfected cells. Data shown is the ratio of ciliated cells after serum feeding relative to baseline. For (B and C), the data represents 3 independent experiments. Cilia were manually

counted, and a minimum of 300 cells was counted for each experimental condition. Error bars are S.E.M. and the p-values were calculated by unpaired Student's t-test.

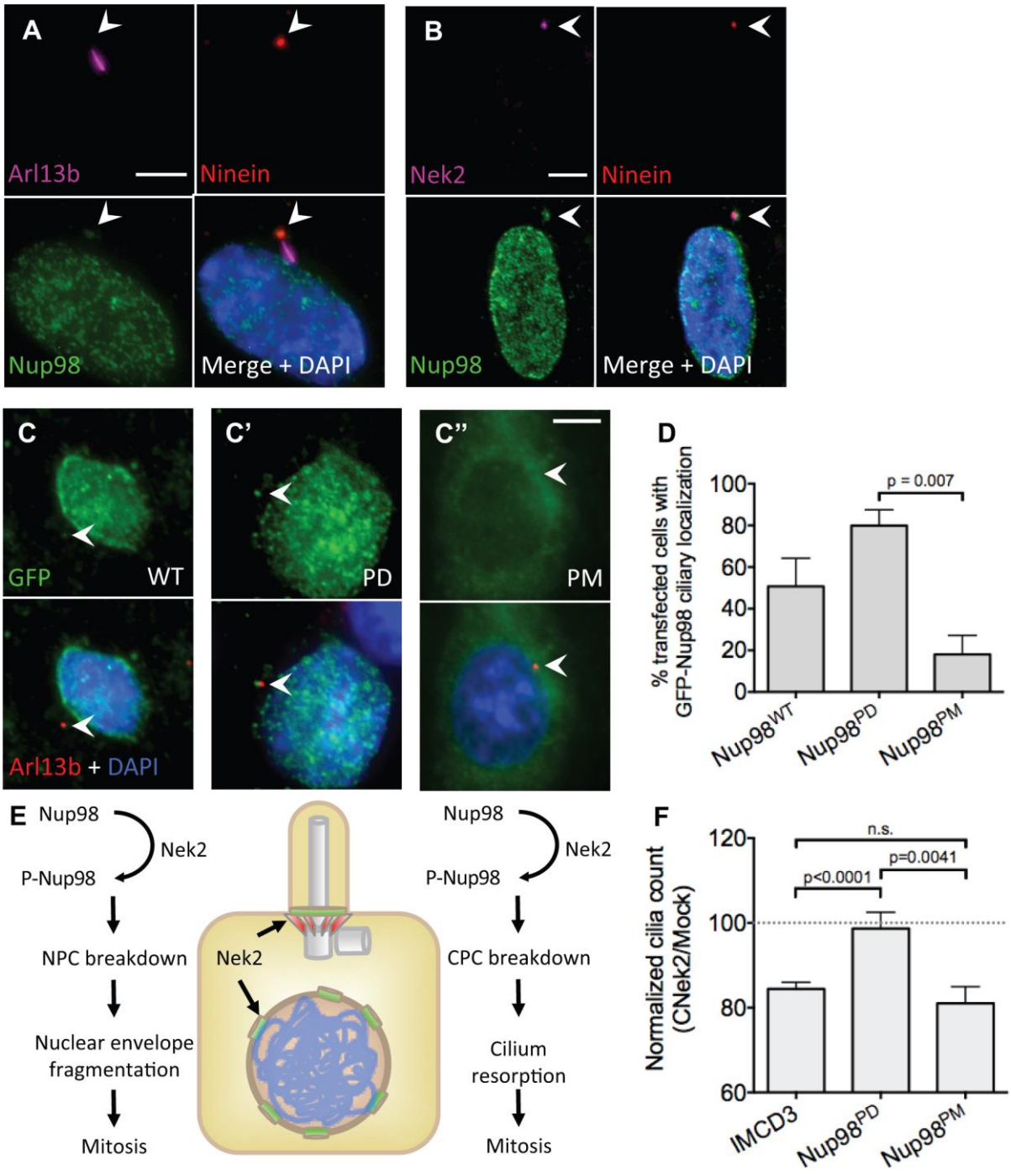

Figure 6. Nup98 localizes to the base of the cilium and influences Nek2-mediated cilium resorption. (A) RPE1 cells stained with a Nup98 antibody show punctate staining across the nuclear envelope and a single focus of staining at the base of the cilium overlapping with the mother centriole marker Ninein. Only the ~33% of cells that had the cilium positioned

distinctly from the nuclear envelope were counted. An average of 42%-75% of cells that were scored had Nup98 at the base of the cilium. (B) In interphase cells, Nek2 colocalizes with Nup98 and Ninein. (C) EGFP-tagged Nup98 localizes to the nuclear envelope and to the base of the cilium. (C') PD Nup98 strongly localizes to the nucleus and base of the cilium, while (C'') PM Nup98 has a more diffuse localization. (D) Percentages of transfected cells with GFP-Nup98 staining at the ciliary base. This experiment was performed 3 times. (E) Model of hypothesized involvement of Nek2 and Nup98 in cilia resorption (F) An IMCD3 stable line expressing a Nup98 (PD) construct is significantly more resistant to Nek2 mediated cilium resorption than the parent line or a line stably expressing Nup98 (PM). The normalized cilia count is the ratio between cilia number in transfected cells divided by cilia count in mock transfected cells. This experiment was performed 5 times, counting ~1000 cells each time. Error bars are S.E.M. p-values were calculated by Student's t-test. Scale bars = 10 μm.

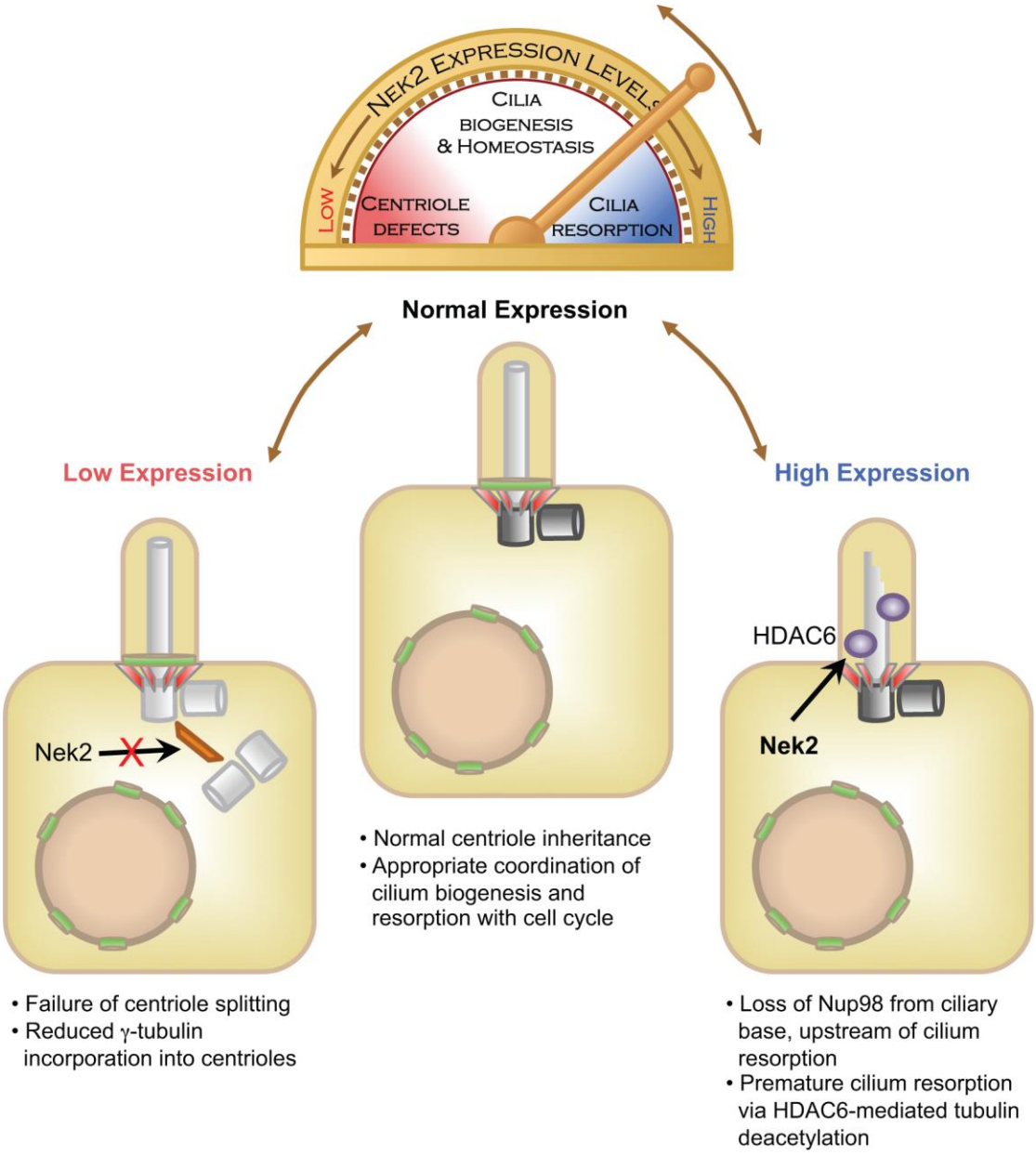

Figure 7. Model of the roles of Nek2 in cilia biogenesis and resorption. Nek2 expression levels are important for cilium homeostasis. Overexpression of Nek2 leads to premature resorption, while reduced expression results in a failure of cilium biogenesis. Lower panels are images of cells with low expression, normal expression, and high expression. One the diagrams, nucleoporins are shown in green; centrioles are in gray; HDAC6 is in purple; centriole appendages are in red.

References

Bahe, S., Stierhof, Y.D., Wilkinson, C.J., Leiss, F., and Nigg, E.A. (2005). Rootletin forms centriole-associated filaments and functions in centrosome cohesion. *The Journal of cell biology* **171**, 27-33.

Bayliss, R., Sardon, T., Vernos, I., and Conti, E. (2003). Structural basis of Aurora-A activation by TPX2 at the mitotic spindle. *Molecular cell* **12**, 851-862.

Bellomo, D., Lander, A., Harragan, I., and Brown, N.A. (1996). Cell proliferation in mammalian gastrulation: the ventral node and notochord are relatively quiescent. *Developmental dynamics : an official publication of the American Association of Anatomists* **205**, 471-485.

Blum, M., Beyer, T., Weber, T., Vick, P., Andre, P., Bitzer, E., and Schweickert, A. (2009). Xenopus, an ideal model system to study vertebrate left-right asymmetry. *Developmental dynamics : an official publication of the American Association of Anatomists* **238**, 1215-1225.

Blum, M., Schweickert, A., Vick, P., Wright, C.V., and Danilchik, M.V. (2014). Symmetry breakage in the vertebrate embryo: when does it happen and how does it work? *Developmental biology* **393**, 109-123.

Boskovski, M.T., Yuan, S., Pedersen, N.B., Goth, C.K., Makova, S., Clausen, H., Brueckner, M., and Khokha, M.K. (2013). The heterotaxy gene GALNT11 glycosylates Notch to orchestrate cilia type and laterality. *Nature* **504**, 456-459.

Brito, D.A., Gouveia, S.M., and Bettencourt-Dias, M. (2012). Deconstructing the centriole: structure and number control. *Current opinion in cell biology* **24**, 4-13.

Cahu, J., Olichon, A., Hentrich, C., Schek, H., Drinjakovic, J., Zhang, C., Doherty-Kirby, A., Lajoie, G., and Surrey, T. (2008). Phosphorylation by Cdk1 increases the binding of Eg5 to microtubules in vitro and in Xenopus egg extract spindles. *PloS one* **3**, e3936.

Cajanek, L., and Nigg, E.A. (2014). Cep164 triggers ciliogenesis by recruiting Tau tubulin kinase 2 to the mother centriole. *Proc Natl Acad Sci U S A* **111**, E2841-2850.

Dishinger, J.F., Kee, H.L., Jenkins, P.M., Fan, S., Hurd, T.W., Hammond, J.W., Truong, Y.N., Margolis, B., Martens, J.R., and Verhey, K.J. (2010). Ciliary entry of the kinesin-2 motor KIF17 is regulated by importin-beta2 and RanGTP. *Nature cell biology* **12**, 703-710.

Eckerdt, F., Yamamoto, T.M., Lewellyn, A.L., and Maller, J.L. (2011). Identification of a polo-like kinase 4-dependent pathway for de novo centriole formation. *Current biology : CB* **21**, 428-432.

Fakhro, K.A., Choi, M., Ware, S.M., Belmont, J.W., Towbin, J.A., Lifton, R.P., Khokha, M.K., and Brueckner, M. (2011). Rare copy number variations in congenital heart disease patients identify unique genes in left-right patterning. *Proc Natl Acad Sci U S A* **108**, 2915-2920.

Faragher, A.J., and Fry, A.M. (2003). Nek2A kinase stimulates centrosome disjunction and is required for formation of bipolar mitotic spindles. *Molecular biology of the cell* **14**, 2876-2889.

Fry, A.M., Descombes, P., Twomey, C., Bacchieri, R., and Nigg, E.A. (2000). The NIMA-related kinase X-Nek2B is required for efficient assembly of the zygotic centrosome in Xenopus laevis. *Journal of cell science* **113 (Pt 11)**, 1973-1984.

Fry, A.M., Mayor, T., Meraldi, P., Stierhof, Y.D., Tanaka, K., and Nigg, E.A. (1998a). C-Nap1, a novel centrosomal coiled-coil protein and candidate substrate of the cell cycle-regulated protein kinase Nek2. *The Journal of cell biology* **141**, 1563-1574.
Fry, A.M., Meraldi, P., and Nigg, E.A. (1998b). A centrosomal function for the human Nek2 protein kinase, a member of the NIMA family of cell cycle regulators. *The EMBO journal* **17**, 470-481.
Fry, A.M., O'Regan, L., Sabir, S.R., and Bayliss, R. (2012). Cell cycle regulation by the NEK family of protein kinases. *Journal of cell science* **125**, 4423-4433.
Fry, A.M., Schultz, S.J., Bartek, J., and Nigg, E.A. (1995). Substrate specificity and cell cycle regulation of the Nek2 protein kinase, a potential human homolog of the mitotic regulator NIMA of Aspergillus nidulans. *The Journal of biological chemistry* **270**, 12899-12905.
Hamada, H., Meno, C., Saijoh, Y., Adachi, H., Yashiro, K., Sakuma, R., and Shiratori, H. (2001). Role of asymmetric signals in left-right patterning in the mouse. *Am J Med Genet* **101**, 324-327.
Hamada, H., and Tam, P.P. (2014). Mechanisms of left-right asymmetry and patterning: driver, mediator and responder. *F1000prime reports* **6**, 110.
Hames, R.S., and Fry, A.M. (2002). Alternative splice variants of the human centrosome kinase Nek2 exhibit distinct patterns of expression in mitosis. *The Biochemical journal* **361**, 77-85.
Hashizume, C., Moyori, A., Kobayashi, A., Yamakoshi, N., Endo, A., and Wong, R.W. (2013). Nucleoporin Nup62 maintains centrosome homeostasis. *Cell cycle* **12**, 3804-3816.
Hubbert, C., Guardiola, A., Shao, R., Kawaguchi, Y., Ito, A., Nixon, A., Yoshida, M., Wang, X.F., and Yao, T.P. (2002). HDAC6 is a microtubule-associated deacetylase. *Nature* **417**, 455-458.
Hurd, T.W., Fan, S., and Margolis, B.L. (2011). Localization of retinitis pigmentosa 2 to cilia is regulated by Importin beta2. *Journal of cell science* **124**, 718-726.
Isao Shiraishi, H.I. (2012). Human Heterotaxy Sundrome. *Circulation Journal of the Japanese Circulation Society* **76**, 2066-2075.
Ishikawa, H., Kubo, A., Tsukita, S., and Tsukita, S. (2005). Odf2-deficient mother centrioles lack distal/subdistal appendages and the ability to generate primary cilia. *Nature cell biology* **7**, 517-524.
Itoh, G., Sugino, S., Ikeda, M., Mizuguchi, M., Kanno, S., Amin, M.A., Iemura, K., Yasui, A., Hirota, T., and Tanaka, K. (2013). Nucleoporin Nup188 is required for chromosome alignment in mitosis. *Cancer science* **104**, 871-879.
Kee, H.L., Dishinger, J.F., Blasius, T.L., Liu, C.J., Margolis, B., and Verhey, K.J. (2012). A size-exclusion permeability barrier and nucleoporins characterize a ciliary pore complex that regulates transport into cilia. *Nature cell biology* **14**, 431-437.
Kennedy, M.P., Omran, H., Leigh, M.W., Dell, S., Morgan, L., Molina, P.L., Robinson, B.V., Minnix, S.L., Olbrich, H., Severin, T., *et al.* (2007). Congenital heart disease and other heterotaxic defects in a large cohort of patients with primary ciliary dyskinesia. *Circulation* **115**, 2814-2821.
Khokha, M.K., Chung, C., Bustamante, E.L., Gaw, L.W., Trott, K.A., Yeh, J., Lim, N., Lin, J.C., Taverner, N., Amaya, E., *et al.* (2002). Techniques and probes for the study of Xenopus tropicalis development. *Developmental dynamics : an official publication of the American Association of Anatomists* **225**, 499-510.
Kim, M., Kim, M., Lee, M.S., Kim, C.H., and Lim, D.S. (2014). The MST1/2-SAV1 complex of the Hippo pathway promotes ciliogenesis. *Nature communications* **5**, 5370.
Kim, S., Lee, K., Choi, J.H., Ringstad, N., and Dynlacht, B.D. (2015). Nek2 activation of Kif24 ensures cilium disassembly during the cell cycle. *Nature communications* **6**, 8087.

Kinzel, D., Boldt, K., Davis, E.E., Burtscher, I., Trumbach, D., Diplas, B., Attie-Bitach, T., Wurst, W., Katsanis, N., Ueffing, M., *et al.* (2010). Pitchfork regulates primary cilia disassembly and left-right asymmetry. *Developmental cell* **19**, 66-77.
Laurell, E., Beck, K., Krupina, K., Theerthagiri, G., Bodenmiller, B., Horvath, P., Aebersold, R., Antonin, W., and Kutay, U. (2011). Phosphorylation of Nup98 by multiple kinases is crucial for NPC disassembly during mitotic entry. *Cell* **144**, 539-550.
Levin, M., Johnson, R.L., Stern, C.D., Kuehn, M., and Tabin, C. (1995). A molecular pathway determining left-right asymmetry in chick embryogenesis. *Cell* **82**, 803-814.
Li, A., Saito, M., Chuang, J.Z., Tseng, Y.Y., Dedesma, C., Tomizawa, K., Kaitsuka, T., and Sung, C.H. (2011). Ciliary transition zone activation of phosphorylated Tctex-1 controls ciliary resorption, S-phase entry and fate of neural progenitors. *Nature cell biology* **13**, 402-411.
Li, Y., Klena, N.T., Gabriel, G.C., Liu, X., Kim, A.J., Lemke, K., Chen, Y., Chatterjee, B., Devine, W., Damerla, R.R., *et al.* (2015). Global genetic analysis in mice unveils central role for cilia in congenital heart disease. *Nature*.
Man, X., Megraw, T.L., and Lim, Y.P. (2015). Cep68 can be regulated by Nek2 and SCF complex. *European journal of cell biology* **94**, 162-172.
Mardin, B.R., Lange, C., Baxter, J.E., Hardy, T., Scholz, S.R., Fry, A.M., and Schiebel, E. (2010). Components of the Hippo pathway cooperate with Nek2 kinase to regulate centrosome disjunction. *Nature cell biology* **12**, 1166-1176.
McGrath, J., Somlo, S., Makova, S., Tian, X., and Brueckner, M. (2003). Two populations of node monocilia initiate left-right asymmetry in the mouse. *Cell* **114**, 61-73.
Moe R. Mahjoub, M.Q.R., Lynne M. Quarmby (2004). A NIMA-related kinase, Fa2p, localizes to a novel site in the proximal cilia of Chlamydomonas and mouse kidney cells. *Molecular Biology of the Cell* **15**, 5172-5286.
Nakamura, T., Saito, D., Kawasumi, A., Shinohara, K., Asai, Y., Takaoka, K., Dong, F., Takamatsu, A., Belo, J.A., Mochizuki, A., *et al.* (2012). Fluid flow and interlinked feedback loops establish left-right asymmetric decay of Cerl2 mRNA. *Nature communications* **3**, 1322.
Nonaka, S., Shiratori, H., Saijoh, Y., and Hamada, H. (2002). Determination of left-right patterning of the mouse embryo by artificial nodal flow. *Nature* **418**, 96-99.
Nonaka, S., Tanaka, Y., Okada, Y., Takeda, S., Harada, A., Kanai, Y., Kido, M., and Hirokawa, N. (1998). Randomization of left-right asymmetry due to loss of nodal cilia generating leftward flow of extraembryonic fluid in mice lacking KIF3B motor protein [published erratum appears in Cell 1999 Oct 1;99(1):117]. *Cell* **95**, 829-837.
Otto, E.A., Trapp, M.L., Schultheiss, U.T., Helou, J., Quarmby, L.M., and Hildebrandt, F. (2008). NEK8 mutations affect ciliary and centrosomal localization and may cause nephronophthisis. *Journal of the American Society of Nephrology : JASN* **19**, 587-592.
Pugacheva, E.N., Jablonski, S.A., Hartman, T.R., Henske, E.P., and Golemis, E.A. (2007). HEF1-dependent Aurora A activation induces disassembly of the primary cilium. *Cell* **129**, 1351-1363.
Schweickert, A., Vick, P., Getwan, M., Weber, T., Schneider, I., Eberhardt, M., Beyer, T., Pachur, A., and Blum, M. (2010). The nodal inhibitor Coco is a critical target of leftward flow in Xenopus. *Current biology : CB* **20**, 738-743.
Schweickert, A., Weber, T., Beyer, T., Vick, P., Bogusch, S., Feistel, K., and Blum, M. (2007). Cilia-driven leftward flow determines laterality in Xenopus. *Current biology : CB* **17**, 60-66.
Sonn, S., Khang, I., Kim, K., and Rhee, K. (2004). Suppression of Nek2A in mouse early embryos confirms its requirement for chromosome segregation. *Journal of cell science* **117**, 5557-5566.

Spalluto, C., Wilson, D.I., and Hearn, T. (2012). Nek2 localises to the distal portion of the mother centriole/basal body and is required for timely cilium disassembly at the G2/M transition. *European journal of cell biology* **91**, 675-686.
Sulik, K., Dehart, D.B., Iangaki, T., Carson, J.L., Vrablic, T., Gesteland, K., and Schoenwolf, G.C. (1994). Morphogenesis of the murine node and notochordal plate. *Developmental dynamics : an official publication of the American Association of Anatomists* **201**, 260-278.
Supp, D.M., Brueckner, M., Kuehn, M.R., Witte, D.P., Lowe, L.A., McGrath, J., Corrales, J., and Potter, S.S. (1999). Targeted deletion of the ATP binding domain of left-right dynein confirms its role in specifying development of left-right asymmetries. *Development* **126**, 5495-5504.
Supp, D.M., Witte, D.P., Potter, S.S., and Brueckner, M. (1997). Mutation of an axonemal dynein affects left-right asymmetry in inversus viscerum mice. *Nature* **389**, 963-966.
Sutherland, M.J., and Ware, S.M. (2009). Disorders of left-right asymmetry: heterotaxy and situs inversus. *American journal of medical genetics Part C, Seminars in medical genetics* **151C**, 307-317.
Takao, D., Dishinger, J.F., Kee, H.L., Pinskey, J.M., Allen, B.L., and Verhey, K.J. (2014). An assay for clogging the ciliary pore complex distinguishes mechanisms of cytosolic and membrane protein entry. *Current biology : CB* **24**, 2288-2294.
Takitoh, T., Kumamoto, K., Wang, C.C., Sato, M., Toba, S., Wynshaw-Boris, A., and Hirotsune, S. (2012). Activation of Aurora-A is essential for neuronal migration via modulation of microtubule organization. *The Journal of neuroscience : the official journal of the Society for Neuroscience* **32**, 11050-11066.
Thiel, C., Kessler, K., Giessl, A., Dimmler, A., Shalev, S.A., von der Haar, S., Zenker, M., Zahnleiter, D., Stoss, H., Beinder, E., *et al.* (2011). NEK1 mutations cause short-rib polydactyly syndrome type majewski. *American journal of human genetics* **88**, 106-114.
Trieselmann, N., Armstrong, S., Rauw, J., and Wilde, A. (2003). Ran modulates spindle assembly by regulating a subset of TPX2 and Kid activities including Aurora A activation. *Journal of cell science* **116**, 4791-4798.
Tucker, R.W., Pardee, A.B., and Fujiwara, K. (1979). Centriole ciliation is related to quiescence and DNA synthesis in 3T3 cells. *Cell* **17**, 527-535.
Uetake, Y., Loncarek, J., Nordberg, J.J., English, C.N., La Terra, S., Khodjakov, A., and Sluder, G. (2007). Cell cycle progression and de novo centriole assembly after centrosomal removal in untransformed human cells. *The Journal of cell biology* **176**, 173-182.
Vonica, A., and Brivanlou, A.H. (2007). The left-right axis is regulated by the interplay of Coco, Xnr1 and derriere in Xenopus embryos. *Developmental biology* **303**, 281-294.
Wloga, D., Camba, A., Rogowski, K., Manning, G., Jerka-Dziadosz, M., and Gaertig, J. (2006). Members of the NIMA-related kinase family promote disassembly of cilia by multiple mechanisms. *Molecular biology of the cell* **17**, 2799-2810.
Wu, X., Kasper, L.H., Mantcheva, R.T., Mantchev, G.T., Springett, M.J., and van Deursen, J.M. (2001). Disruption of the FG nucleoporin NUP98 causes selective changes in nuclear pore complex stoichiometry and function. *Proc Natl Acad Sci U S A* **98**, 3191-3196.
Yuan, S., Zaidi, S., and Brueckner, M. (2013). Congenital heart disease: emerging themes linking genetics and development. *Curr Opin Genet Dev* **23**, 352-359.
Yuan, S., Zhao, L., Brueckner, M., and Sun, Z. (2015). Intraciliary calcium oscillations initiate vertebrate left-right asymmetry. *Current biology : CB* **25**, 556-567.

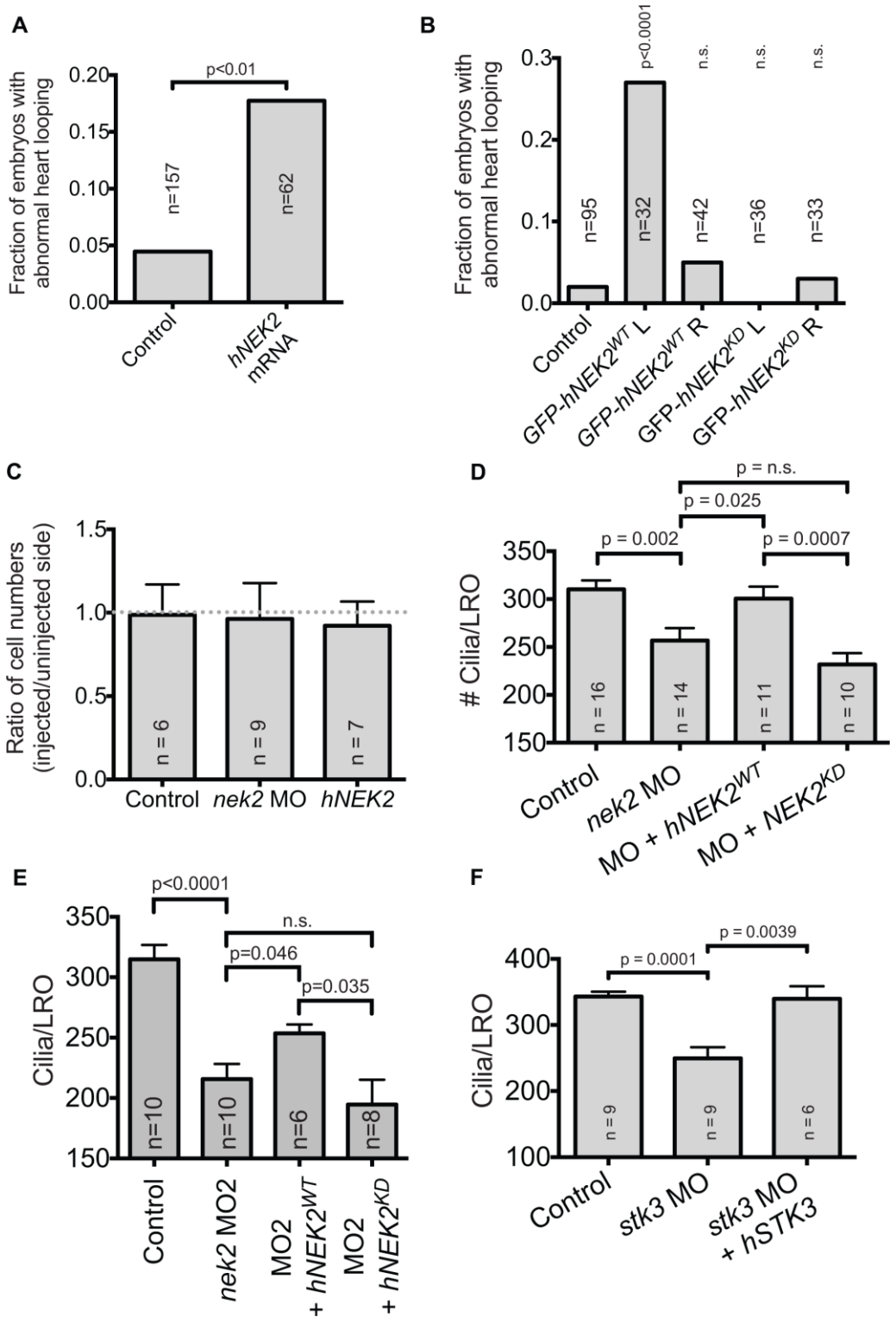

Fig. S1. Nek2 overexpression causes a heart-looping phenotype in *Xenopus*, dependent on its kinase activity. (A). Nek2 overexpression in *Xenopus* results in abnormal heart-looping. (B) Overexpression of Nek2 on the left causes abnormal heart-looping, while overexpression on the right does not, consistent with an LRO cilia phenotype.

Overexpression of an equal amount of kinase-dead Nek2 does not cause a cardiac-looping phenotype. (C) Knockdown or overexpression of Nek2 does not affect cell numbers in the LRO of unilaterally-injected embryos. (D) Injection of WT h*NEK2* mRNA is able to rescue LRO cilia loss from MO1; however, injection of kinase-dead h*NEK2* is unable to rescue. (E) Injection of WT *hNEK2* mRNA is able to rescue LRO cilia loss from MO2; however, injection of kinase-dead *hNEK2* is unable to rescue. (F) Injection of *hSTK3* mRNA is able to rescue cilia loss from the LRO caused by MO-mediated knockdown of *stk3*. For (A-B) p-values were calculated by χ^2 test. For (C) all p-values are non-significant, calculated by paired t-test. For (D-F) error bars are S.E.M. p-values were calculated by unpaired Student's t-test.

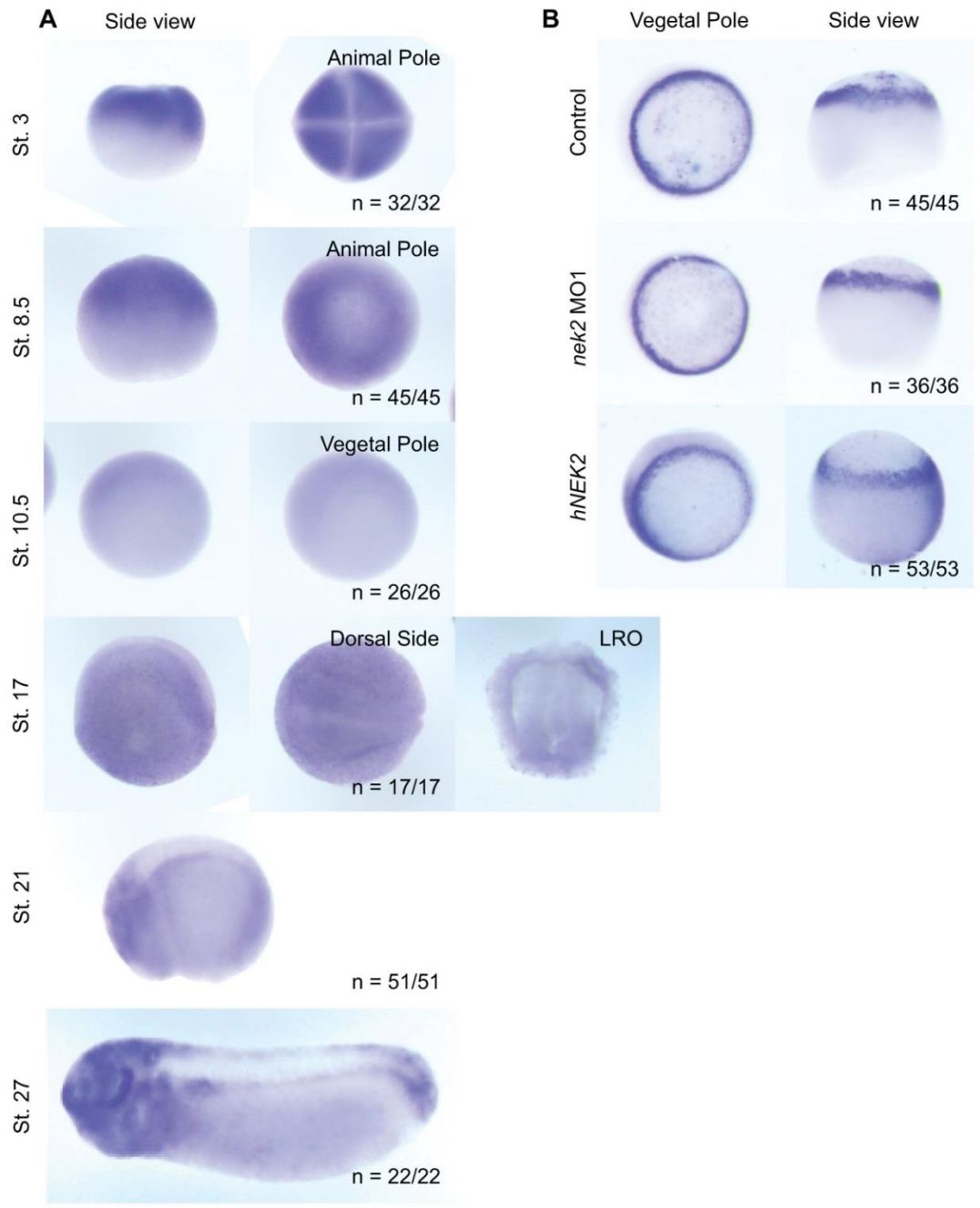

Fig. S2. *nek2* is expressed in many tissues involved in LR patterning. (A) *nek2* is expressed ubiquitously in early stage embryos, but at higher levels in the tissues with more rapidly dividing cells (the animal pole). *nek2* is expressed in the LRO (st. 16-17), the mediolateral midline (st. 21 & st. 27) and the lateral plate mesoderm (st. 21). (B) Neither knockdown nor overexpression of Nek2 affect mesoderm specification during gastrulation, suggesting that the LRO cilia defect does not arise from an improper specification of superficial mesoderm.

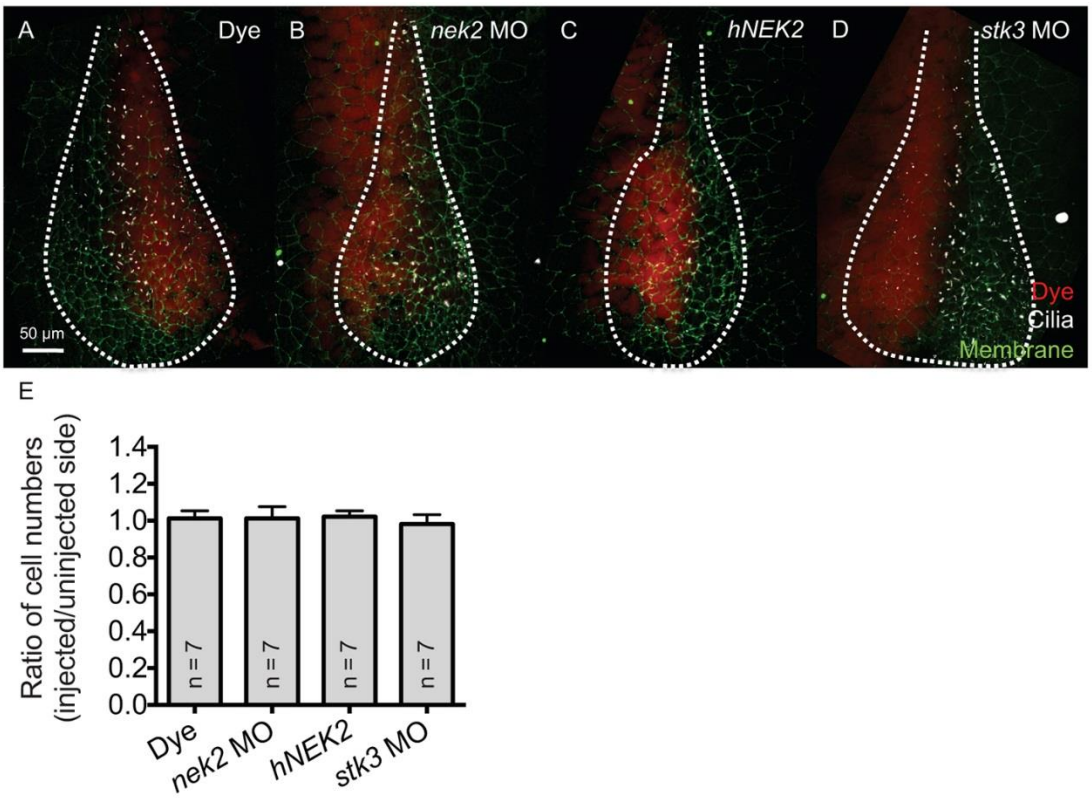

Fig. S3. *stk3* knockdown and *nek2* knockdown and overexpression do not affect cell numbers in the LRO. 2-cell *Xenopus* embryos were injected unilaterally with dye (A), *nek2* MO1 (B), *hNEK2* mRNA (C), or *stk3* MO (D), and immuno-labeled for acetylated tubulin (cilia) and cadherin (membrane). The LRO tissue is outlined in a white dotted line. There were no changes in cell number between the injected and uninjected sides (E).

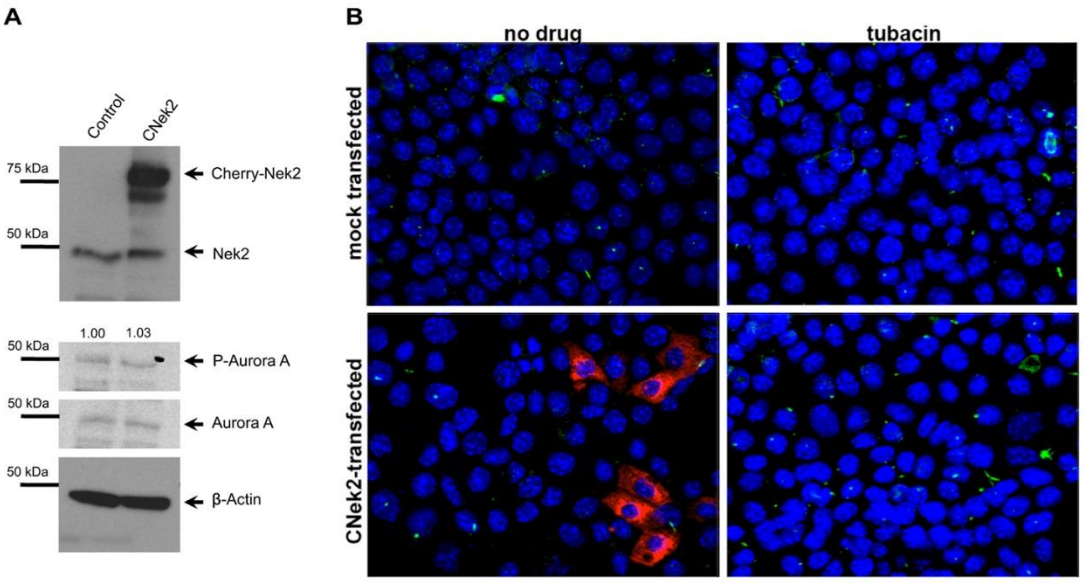

Fig. S4. Overexpression of Cherry-Nek2 in cultured cells does not affect levels of Aurora A phosphorylation. (A) Western blot showing levels of Nek2, Aurora A, P-Aurora A, with a GAPDH loading control. The quantification shown is the intensity of the PAA band divided by the intensity of the AA band, and then normalized to the mock transfected control. This experiment was completed 5 times with similar results. (B) Representative panels of cultured IMCD3 cells treated with tubacin showing level of ciliation. Cells are immuno-labeled for acetylated tubulin (cilia, green) and counterstained with Hoechst nuclear dye (blue). CNek2 transfected cells are immuno-labeled for DS-Red in the lower left panel.

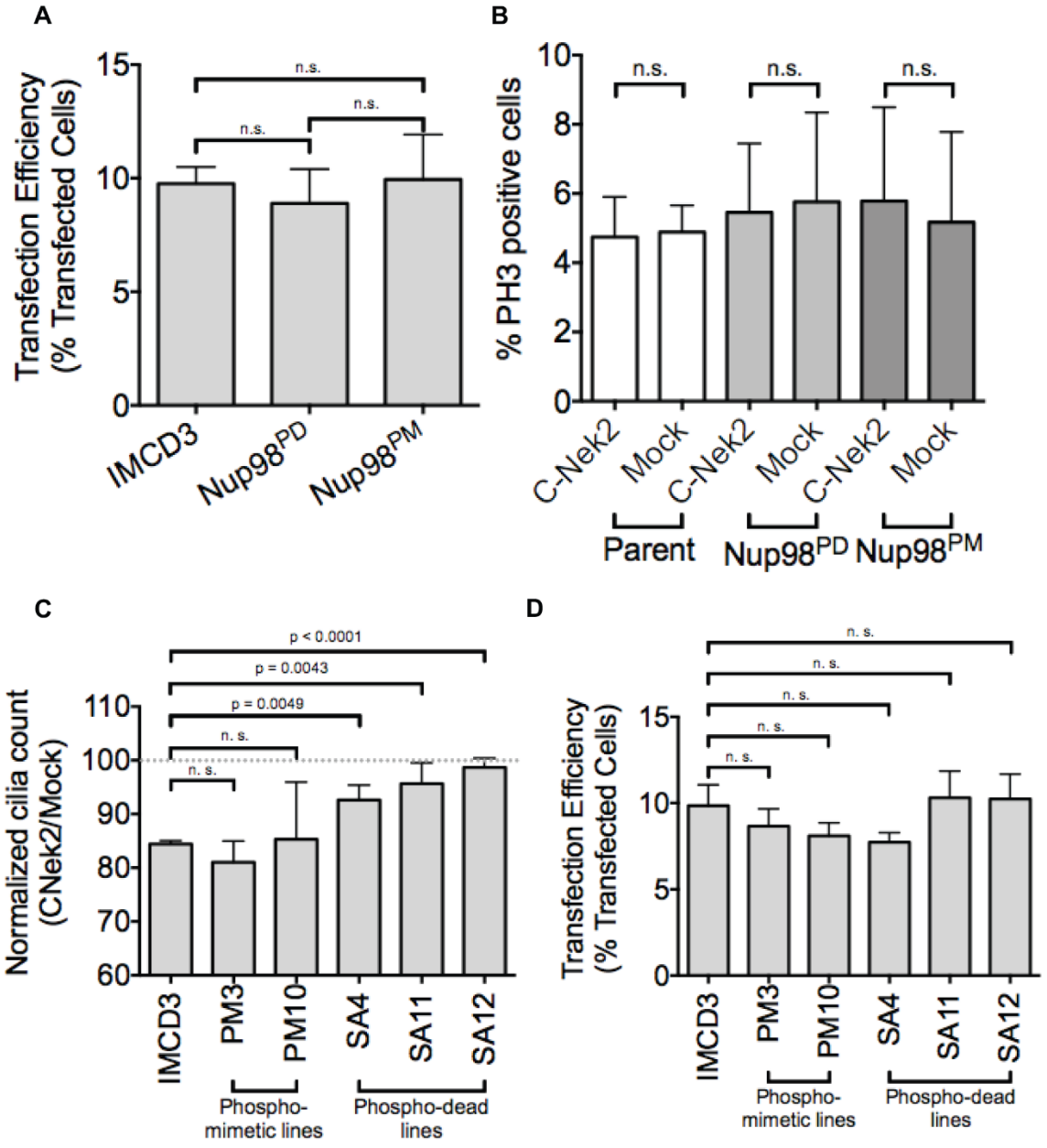

Fig. S5. NUP98 influences NEK2-mediated cilium resorption. (A) All cell lines in Figure 6F have the same transfection efficiency. (B) Transfection of the cell lines shown in Figure 6F does not influence mitotic index. (C) Multiple lines expressing PD Nup98 are resistant to Nek2-mediate cilium resorption, while lines expressing PM Nup98 are not. (D) None of the lines from (C) show different transfection efficiency from the parent line.